THE JOURNAL OF BIOLOGICAL CHEMISTRY VOL. 288, NO. 34, pp. 24394–24409, August 23, 2013

The Galectin CvGal1 from the Eastern Oyster (*Crassostrea virginica*) Binds to Blood Group A Oligosaccharides on the Hemocyte Surface*[S]

Received for publication, April 18, 2013, and in revised form, June 19, 2013 Published, JBC Papers in Press, July 3, 2013, DOI 10.1074/jbc.M113.476531

Chiguang Feng[‡], Anita Ghosh[§], Mohammed N. Amin[¶], Barbara Giomarelli[‡], Surekha Shridhar[‡], Aditi Banerjee[‡], José A. Fernández-Robledo[‡1], Mario A. Bianchet[§], Lai-Xi Wang[¶], Iain B. H. Wilson[‖], and Gerardo R. Vasta[‡2]

From the [‡]Department of Microbiology and Immunology, University of Maryland School of Medicine and Institute of Marine and Environmental Technology, Baltimore, Maryland 21202, the [§]Department of Neurology, The Johns Hopkins University School of Medicine, Baltimore, Maryland 21205, the [¶]Institute of Human Virology, Department of Biochemistry and Molecular Biology, University of Maryland School of Medicine, Baltimore, Maryland 21201, and the [‖]Department für Chemie, Universität für Bodenkultur, A-1190 Wien, Austria

Background: The carbohydrate specificity of the oyster galectin CvGal1 for endogenous and exogenous glycans was unresolved.
Results: CvGal1 recognizes blood group A tetrasaccharides on oyster hemocytes, which are absent on the surface of the *P. marinus* parasite.
Conclusion: Oyster hemocytes and *P. marinus* display structurally distinct ligands for CvGal1.
Significance: Galectins may function as pattern recognition receptors by binding microbial glycans structurally different from endogenous ligands.

The galectin CvGal1 from the eastern oyster (*Crassostrea virginica*), which possesses four tandemly arrayed carbohydrate recognition domains, was previously shown to display stronger binding to galactosamine and *N*-acetylgalactosamine relative to D-galactose. CvGal1 expressed by phagocytic cells is "hijacked" by the parasite *Perkinsus marinus* to enter the host, where it proliferates and causes systemic infection and death. In this study, a detailed glycan array analysis revealed that CvGal1 preferentially recognizes type 2 blood group A oligosaccharides. Homology modeling of the protein and its oligosaccharide ligands supported this preference over type 1 blood group A and B oligosaccharides. The CvGal ligand models were further validated by binding, inhibition, and competitive binding studies of CvGal1 and ABH-specific monoclonal antibodies with intact and deglycosylated glycoproteins, hemocyte extracts, and intact hemocytes and by surface plasmon resonance analysis. A parallel glycomic study carried out on oyster hemocytes (Kurz, S., Jin, C., Hykollari, A., Gregorich, D., Giomarelli, B., Vasta, G. R., Wilson, I. B. H., and Paschinger, K. (2013) *J. Biol. Chem.* 288,) determined the structures of oligosaccharides recognized by CvGal1. Proteomic analysis of the hemocyte glycoproteins identified β-integrin and dominin as CvGal1 "self"-ligands. Despite strong CvGal1 binding to *P. marinus* trophozoites, no binding of ABH blood group antibodies was observed. Thus, parasite glycans structurally distinct from the blood group A oligosaccharides on the hemocyte surface may function as potentially effective ligands for CvGal1. We hypothesize that carbohydrate-based mimicry resulting from the host/parasite co-evolution facilitates CvGal1-mediated cross-linking to β-integrin, located on the hemocyte surface, leading to cell activation, phagocytosis, and host infection.

Invertebrates lack the typical adaptive immune responses of vertebrates, but they display effective innate immunity for defense against microbial infection (1). Among the multiple factors involved in recognition of the potential infectious challenges, a diversified repertoire of soluble and cell-associated lectins mediate binding interactions with potential pathogens that usually result in their agglutination, immobilization, and phagocytosis or encapsulation by hemolymph cells (hemocytes) (2). The engulfed microbe is killed by oxidative stress resulting from the respiratory burst by the hemocytes upon particle uptake and is degraded in the phagosomal compartment (3).

The eastern oyster *Crassostrea virginica* is a keystone species in the Chesapeake Bay and other coastal areas of North America (4). As active filter feeders, oysters are critical components of the estuarine ecosystems that contribute to maintain water quality and environmental health overall (5). Like most invertebrates, eastern oysters have a diverse lectin repertoire present in plasma and phagocytic hemocytes (6, 7) and are able to effectively respond to most immune challenges (4). Nevertheless, the protozoan parasite *Perkinsus marinus* successfully infects and causes "Dermo" disease in the eastern oyster (8, 9). Since the 1950s, it has produced extensive damage to oyster bars along the Gulf of Mexico and Atlantic coast, with catastrophic

* This work was supported, in whole or in part, by National Institutes of Health Grants 5R01GM070589-06 (to G. R. V.) and R01 GM080374 (to L. X. W.). This work was also supported by Grants IOS-0822257 and IOS-1063729 from the National Science Foundation.
[S] This article contains supplemental Figs. S1–S5.
[1] Present address: Bigelow Laboratory for Ocean Sciences, P. O. Box 380, 60 Bigelow Dr., East Boothbay, ME 04544.
[2] To whom correspondence should be addressed: Dept. of Microbiology and Immunology, University of Maryland School of Medicine, and Institute of Marine and Environmental Technology, Columbus Center, 701 East Pratt St., Baltimore, MD 21202. Tel.: 410-234-8826; Fax: 410-234-8896; E-mail: GVasta@som.umaryland.edu.

consequences for local fisheries and the health of coastal waters (10). Recent reports indicate that oyster populations from the Pacific coast of North America are also affected (11). Transmission of Dermo disease is not fully understood but is thought to occur mainly through the release into the water column of *P. marinus* trophozoites from infected oysters (12). Trophozoites are filtered by neighboring oysters, and once in contact with the mantle, gills, and the gut lumen, they are phagocytosed by hemocytes, which migrate into the internal milieu (12, 13). The phagocytosed trophozoites survive intracellular killing and proliferate. Therefore, the hemocytes provide not only the means of parasite uptake and entry but also an environment favorable for parasite proliferation and dissemination, leading to systemic infection and death of the oyster (14). The cell entry mechanisms of *P. marinus* have not been fully elucidated, but in a previous study, we identified a galectin (CvGal1)[3] of unique structure that plays a significant role in entering the host hemocytes (15).

Galectins are lectins characterized by their binding affinity for β-galactosides, a unique binding site sequence motif, and wide taxonomic distribution and structural conservation in vertebrates, invertebrates, protista, and fungi (16). They not only bind endogenous ("self") glycans and mediate developmental processes and cancer metastasis (17), but they also function as key regulators of both innate and adaptive immune responses (18). More recently, however, evidence has accumulated to reveal that galectins also bind exogenous ("non-self") glycans on the surface of potentially pathogenic microbes, parasites, and fungi, suggesting that galectins can function as pattern recognition receptors (PRRs) in innate immunity (19). According to the currently accepted model for non-self recognition, PRRs recognize pathogens via highly conserved microbial surface molecules of wide distribution (pathogen-associated molecular patterns), such as LPS or peptidoglycans, which are absent in the host (20). Galectins, however, apparently bind similar self and non-self molecular patterns (galactoside-containing glycans) on host and microbial cells. This apparent paradox underscores the significant gaps in our knowledge about the structural and biophysical aspects of the interactions of galectins with endogenous and microbial carbohydrate moieties (20).

In addition to binding self glycans on the hemocyte surface, CvGal1 also recognizes a variety of potential microbial pathogens and unicellular algae, but it binds preferentially and in a carbohydrate-specific manner to *P. marinus* trophozoites (15). Attachment and spreading of oyster hemocytes to foreign surfaces induce localization of CvGal1 to the cell periphery, its secretion and binding to the plasma membrane, and the release of remaining free CvGal1 to the extracellular compartment. Exposure of oyster hemocytes to *P. marinus* trophozoites or to glycoproteins that behave as strong CvGal1 ligands leads to hemocyte activation and enhances this process further. Partial inhibition of *P. marinus* phagocytosis by pretreatment of oyster hemocytes with anti-CvGal1 antibodies strongly suggests that CvGal1-mediated recognition of *P. marinus* at the hemocyte cell surface is critical for entry of the parasite into the host cells. Our results suggested that the unusual four-CRD organization of CvGal1 facilitates cross-linking of the recognized microbes and unicellular algae to the hemocyte cell surface, thereby promoting phagocytosis, killing, and digestion of the potential infectious challenge and selected components of ingested phytoplankton. However, *P. marinus* trophozoites display a glycocalyx that is selectively recognized by CvGal1 over the abovementioned particles and subverts the host's innate immune/feeding recognition mechanism to gain entry into those cells that will enable its proliferation and dissemination (15). Thus, the paradox of self *versus* non-self recognition by galectins is even more intriguing for CvGal1 because it is likely to involve host-parasite reciprocal recognition (21).

The biological relevance of the apparent stronger binding of CvGal1 to GalNAc rather than Gal (15) was unclear, and it became of great interest to examine in detail the carbohydrate specificity of CvGal1, identify its binding partners on the oyster hemocyte membrane, and determine whether the same ligands are also present on the parasite surface. In this study, we used multiple approaches to reveal that CvGal1 recognizes blood group A oligosaccharides, also shown in a parallel glycomic study (61) to be present on the oyster hemocyte glycans. Finally, by proteomic analysis, we identified β-integrin and dominin among the hemocyte glycoproteins that are recognized by CvGal1. Although our data indicate that the glycocalyx of *P. marinus* trophozoites contains no blood group A moieties, GalNAc residues are present in surface glycans that are equally good ligands for CvGal1. Thus, we hypothesize that glycan-based mimicry developed by convergent host/parasite evolution enables the parasite to infect oyster hemocytes.

EXPERIMENTAL PROCEDURES

Reagents—Carbohydrates (monosaccharides, oligosaccharides, and glycoproteins, at the highest purity available), α-L-fucosidase (from bovine kidney), neuraminidase (from *Clostridium perfringens*, type V), FITC-labeled concanavalin A (ConA), *Arachis hypogaea* lectin (PNA), and *Ulex europaeus* lectin (UEA) were purchased from Sigma-Aldrich. PNGase F (from *Flavobacterium meningosepticum*), *O*-glycosidase (cloned from *Enterococcus faecalis* and expressed in *Escherichia coli*), α-*N*-acetylgalactosaminidase (cloned from *Chryseobacterium meningosepticum* and expressed in *E. coli*), and β1,3-galactosidase (cloned from *Xanthomonas manihotis* and expressed in *E. coli*) were obtained from New England Biolabs (Ipswich, MA). Trypsin (MS grade) was obtained from Promega (Madison, WI). FITC-labeled *Glycine max* lectin (SBA), *Galanthus nivalis* lectin (GNA), or *Triticum vulgaris* lectin (WGA) from EY Laboratories (San Mateo, CA). Neoglycoproteins were obtained from Accurate Chemical and Scientific Corp. (Westbury, NY) (type 2 blood group A tetrasaccharide-bovine serum albumin (BSA), 20 tetrasaccharide units/BSA polypeptide) and V-labs Inc. (Covington, LA) (blood group A trisaccharide-BSA,

[3] The abbreviations used are: CvGal1, *C. virginica* galectin 1; CRD, carbohydrate recognition domain; HBS, HEPES-buffered saline; ConA, concanavalin A; PNA, *A. hypogaea* lectin; UEA, *U. europaeus* lectin; SBA, *G. max* lectin; GNA, *G. nivalis* lectin; WGA, *Triticum vulgaris* lectin; PSM, porcine stomach mucin; OSM, ovine submaxillary mucin; BSM, bovine submaxillary mucin; SPR, surface plasmon resonance; β-mercaptoethanol, 2-ME; PRR, pattern recognition receptors; PNGase F, peptide:*N*-glycosidase F; PDB, Protein Data Bank; rCvGal1, recombinant CvGal1; ASF, asialofetuin.

19 trisaccharide units/BSA polypeptide; and *N*-acetylgalactosamine-BSA, 28 GalNAc units/BSA polypeptide), or Sigma (GalNAc-BSA, 19 GalNAc units/BSA polypeptide). Other neoglycoproteins (GlcNAc-BSA, 35 GlcNAc units/BSA polypeptide, and Gal-BSA, 23 Gal units/BSA polypeptide) were a generous gift from Yuan Chuan Lee (Department of Biology, The Johns Hopkins University, Baltimore, MD). Mouse monoclonal anti-A and anti-B antibodies (Immucor Inc., Norcross, GA) were the generous gift from the University of Maryland Medical Center Blood Bank. The HRP-labeled goat anti-rabbit IgG was obtained from Bio-Rad. DNA primers and the Alexa 488-labeled goat anti-rabbit IgG was obtained from Invitrogen. The specificity of the rabbit anti-CvGal1 purified IgGs was optimized by cross-adsorption and validated as reported elsewhere (15). Protein electrophoresis reagents were purchased from Bio-Rad. Restriction enzymes were acquired from New England Biolabs. Ex-Taq DNA polymerase and dNTPs were from Takara Bio (Otsu, Japan).

Oyster (C. virginica) Hemocytes—Adult eastern oysters, averaging 40–50 g each, were obtained from a local commercial firm and maintained in 20-liter tanks as reported elsewhere (15). To withdraw hemolymph, oysters were notched using a grinding wheel at the anterior side of the shell, close to the adductor muscle, allowed to acclimate for 3 days in the water tank, and bled from the adductor muscle using an 18-gauge needle, and the hemolymph was collected on wet ice (15). Hemocytes from pooled hemolymph samples from 6 to 12 oysters were collected by centrifugation (800 × *g* for 10 min at 4 °C), washed three times in ice-cold HEPES-buffered saline (HBS: 10 mM HEPES, 430 mM NaCl, 10 mM $CaCl_2$, pH 7.3), suspended in HBS containing glutaraldehyde (10 mM), incubated on wet ice for 10 min, washed three times in HBS, and stored at 4 °C until use. As required, fixed hemocytes were incubated with α-*N*-acetylgalactosaminidase (10^3 units/ml as final concentration in G7 buffer) or buffer only at 37 °C for 72 h.

For the preparation of hemocyte extracts, fresh hemolymph samples from 6 to 12 oysters were pooled, and the circulating hemocytes were collected by centrifugation as above. The pellet was resuspended in 1 ml of PBS (10 mM Na_2HPO_4-NaH_2PO_4, 150 mM NaCl, pH 7.8) and sonicated three times for 10 s on ice. The extract was centrifuged to remove insoluble materials; the clear supernatant was collected; the protein concentration was quantified, and the extracts were stored at −20 °C until use. For flow cytometry analyses, the hemocyte suspensions (1×10^7 cells/ml) were fixed with 1% paraformaldehyde in HBS for 30 min on ice, washed three times with HBS, and processed as described below.

Parasite (P. marinus) Trophozoites—Clonal cultures of *P. marinus* established in our laboratory (*P. marinus* strain PRA 240) (22) were propagated as reported earlier (23). Cultures in log phase of growth were harvested, washed three times in HBS, suspended at 4×10^7 cells/ml in HBS, and treated with glutaraldehyde (10 mM) for 30 min on wet ice. The fixed cells were washed three times with HBS and suspended at 4×10^7 cells/ml in HBS for staining and flow cytometry analysis.

General Procedures

Expression and Purification of Recombinant CvGal1 (rCvGal1)—The CvGal1 construct (15) was transformed into *E. coli* BL21 (DE3)-competent cells (Novagen, Billerica, MA), and the expression of rCvGal1 was induced by 0.1 mM isopropyl β-D-thiogalactoside at 23 °C for 16 h in 3 liters of LB medium containing 30 μg/ml kanamycin. The soluble proteins extracted with BugBuster (Novagen), containing 1 mM PMSF and 0.07% β-mercaptoethanol (2-ME), contained most of the recombinant CvGal1 (~80%). This fraction was loaded onto a column packed with 5 ml of lactose-Sepharose (Sigma). After washing the column thoroughly (washing buffer: 1:10 PBS, 0.07% 2-ME (PBS (1:10)/2-ME), the rCvGal1 was eluted with 0.1 M lactose in PBS (1:10)/2-ME. From a 3-liter *E. coli* culture, ~20 mg of rCvGal1 were purified.

Carbamidomethylation of rCvGal1—Purified rCvGal1 (17 mg) was absorbed on 1 ml of DEAE-Sepharose (Sigma) pre-equilibrated with PBS (1:10)/2-ME and incubated for 1 h at 4 °C with slow agitation. The resin was poured into a column, and after extensive washing with PBS (1:10), the column was overlaid with 3 ml of 0.1 M iodoacetamide, 0.1 M lactose and incubated for 1 h at 4 °C in the dark. After washing the column with 50 mM lactose in PBS (1:10), the bound protein (crCvGal1) was eluted with PBS (1:10), 0.5 M NaCl, 0.1 M lactose.

Enzymatic Treatment of Glycoproteins, Hemocyte Extracts, and Intact Hemocytes—Porcine stomach mucin (PSM; 30 μg/ml, final concentration) or hemocyte extract (100 μg/ml) were incubated with PNGase F (25×10^3 units/ml as final concentration in G7 reaction buffer, pH 7.5), *O*-glycosidase (2×10^6 units/ml in G7, pH 7.5), α-*N*-acetylgalactosaminidase (10^3 units/ml in G7, pH 7.5), α-L-fucosidase (1 unit/ml in G6, pH 5.5), β1,3-galactosidase (500 units/ml in G6, pH 5.5), or buffer only (G6 or G7 as control) at 37 °C for 48 h. To prepare desialylated glycoproteins, fetuin, PSM, ovine submaxillary mucin (OSM), or bovine submaxillary mucin (BSM) (10 μg/ml in Tris buffer, pH 5.5) were incubated with neuraminidase (10 milliunits/ml as final concentration) at 37 °C overnight. The neuraminidase-treated glycoproteins were boiled for 10 min to deactivate the enzyme before use. The untreated (fetuin, PSM, OSM, and BSM) and desialylated (asialofetuin, asialo-PSM, asialo-OSM, and asialo-BSM) glycoproteins as well as glycosidase-treated hemocyte extracts were diluted in PBS for coating onto 96-well plates for binding and binding-inhibition assays as described below. Fixed intact hemocytes were incubated with α-*N*-acetylgalactosaminidase (10^3 units/ml) or buffer only at 37 °C for 72 h, incubated with rCvGal1 or anti-blood group A or B monoclonal antibodies, and analyzed by flow cytometry as described below.

Protein Determinations—Protein concentrations were estimated with the protein assay kit I (Bio-Rad) in 96-well flat-bottom plates as described by the manufacturer in the microassay format, using crystalline BSA as a standard. After 5 min of combining protein and dye, the reactions were read at 595 nm on SpectraMax340 Plate Reader (Molecular Devices, Sunnyvale, CA) controlled by SoftmaxPro software, version 1.

Characterization of the Carbohydrate Specificity of rCvGal1

Glycan Array Analysis—Glycan array analysis was carried out at the Core H of the Consortium for Functional Glycomics at Emory University, on version 5.0 of the array printed with 611 glycans in replicates of six. The rCvGal1 (1 mg/ml) was dialyzed against PBS containing 10 mM β-mercaptoethanol (PBS/2-ME) and diluted with PBS/2-ME to 2, 10, 50, or 150 μg/ml before adding onto an array for analysis. The bound rCvGal1 was detected with rabbit anti-CvGal1-purified IgG, followed by a goat anti-rabbit IgG labeled with AlexaFluor 488 (Invitrogen).

Homology Modeling—The oyster galectin CvGal1 was modeled by using the toad *Bufo arenarum* galectin-1 structure (BaGal1, PDB code 1GAN) (24) as a template. Sequence homologies of Cvgal1 with the template (BaGal1) are shown in Table 1. An initial automatic alignment with the program MOE (CGC Inc.) was further improved conserving the maximum number of the galectin archetypical interactions and locating deletions and insertions in permissive regions of the template structure. Three-dimensional models of CvGal1 were built with the homology modeling routine of MOE and manually rebuilt with the program Coot (25). The structures were regularized and minimized using Charmm27-based force field included in MOE. Loops showing significant variations from the template were modeled using the LowMD conformational search in MOE, maintaining the other residues fixed or alternatively tethered. The carbohydrates were built in MOE and minimized using an MMFX94x force field (MOE version 2012.10). Conformations of the carbohydrates were selected in agreement to their minimum conformational potential energy in vacuum.

Solid Phase Binding, Binding Inhibition, and Competitive Inhibition Assays—Solid phase lectin binding assays were carried out as described elsewhere (15, 26). Briefly, 96-well microtiter plates were coated with neoglycoproteins, or untreated or glycosidase-treated authentic glycoproteins (10 μg/ml in PBS), or hemocyte extracts (0.5 μg/ml in PBS) for 3 h at 37 °C. The plates were washed with 0.1% Tween in PBS (PBST) and blocked overnight with 3% BSA in PBS at 4 °C. The plates were washed three times with cold PBS/2-ME and stored at 4 °C. For binding studies, rCvGal1 (100 μl; 0.5 μg/ml in PBS/2-ME) or anti-A or anti-B monoclonal antibodies (1:100 in PBS) were dispensed into the coated plates and incubated for 1 h at 4 °C. For binding-inhibition studies, rCvGal1 (0.2 μg/ml) was preincubated with serial dilutions of PSM, asialo-PSM, OSM, asialo-OSM, BSM, or asialo-BSM (1:3 serial dilutions starting at 100 μg/ml) for 1 h at 4 °C in PBS/2-ME. The rCvGal/inhibitor mixtures were delivered into the coated plates and incubated for 1 h at 4 °C. Controls were the substitutions of the glycan inhibitor solution by PBS and substitution of purified lectin by PBS. After three washes with PBS/2-ME, the plates were fixed with 2% formaldehyde in PBS for 30 min at 37 °C. The wells were washed twice with 100 mM glycine in PBS and three times with PBST. Binding of rCvGal1 was detected by purified rabbit anti-CvGal1 IgG, followed by an HRP-conjugated anti-rabbit antibody. The plates were developed with TMB substrate for 5 min, and the reaction was stopped by adding 1 M HCl. Optical densities at 450 nm were measured on SpectraMax340 Plate Reader (Molecular Devices) controlled by SoftmaxPro software, version 1. All experiments were carried out in triplicate and repeated at least twice. Binding-inhibition results were expressed as the reciprocal percentage binding activity relative to the no-inhibitor added control (100%; no inhibitor added). In competitive inhibition experiments, the coated plates were preincubated with anti-blood group A or anti-blood group B monoclonal antibodies (1:100 in PBS) for 1 h at 4 °C, washed three times before adding the crCvGal1, and the results expressed as indicated above for binding and binding-inhibition experiments. Controls were the substitution of the monoclonal antibody by PBS and substitution of crCvGal1 by PBS.

Surface Plasmon Resonance (SPR) Measurements—Surface plasmon resonance measurements were carried on a BIAcore T100 (GE Healthcare) instrument at 25 °C. Glycoproteins (PSM, fetuin, and asialofetuin) and neoglycoproteins (blood group A tetrasaccharide-BSA, blood group A trisaccharide-BSA, GalNAc-BSA, Gal-BSA, and GlcNAc-BSA) were immobilized on individual CM5 chips in duplicate cells, until reaching 3000 response units by using amine coupling kit provided by the manufacturer. A reference channel was immobilized with ethanolamine. Binding analyses were performed by injecting a solution of crCvGal1 over four cells at 2-fold increasing concentration in 10 mM HEPES, pH 7.4, containing 150 mM NaCl and 0.005% surfactant P20 at a flow rate of 20 μl/min for 2 min, and allowed to dissociate for another 5 min. The surface was regenerated after each cycle by injecting 3 M $MgCl_2$ (aqueous) solution for 3 min at a flow rate of 30 μl/min. Data were collected at the rate of 10 Hz. T-100 BIAcore evaluation software was utilized to subtract appropriate blank reference and to fit the sensorgram globally by applying a 1:1 Langmuir model. Mass transfer effects were checked by the t_c values displayed by the T-100 BIAcore evaluation software. No significant mass transportation effects were observed.

Characterization of CvGal1 Carbohydrate Ligands on Oyster Hemocytes and P. marinus Trophozoites

Flow Cytometry Analysis of CvGal1 Binding to Oyster Hemocytes and Competitive Inhibition Assays—Fixed hemocytes (untreated or α-*N*-acetylgalactosaminidase-treated) or fixed *P. marinus* trophozoites were incubated with 5% BSA in HBS at room temperature for 1 h and subsequently incubated with 0–100 μg/ml of rCvGal1 for 1 h or with anti-A. For binding-inhibition experiments, the rCvGal1 was incubated with increasing concentrations (up to 1000 μg/ml in HBS/BSA) of PSM or ASF for 1 h on ice before adding the mixtures into the tubes containing the fixed hemocytes. For competitive binding experiments, the hemocytes were preincubated with anti-blood group A or anti-blood group B monoclonal antibodies (1:100 in PBS) before adding the crCvGal1. Controls were the substitution of the glycoprotein inhibitor by BSA, monoclonal antibody by PBS, and substitution of crCvGal1 by PBS. The cells were washed three times and stained with 100 μl of rabbit anti-CvGal1 IgG at room temperature for 1 h, followed by incubation with Alexa 488-labeled anti-rabbit IgG for 1 h at room temperature (for CvGal1 detection) or with Alexa 488-labeled anti-mouse IgM (for anti-A detection). After three washes in HBS, the stained cells were analyzed with Accuri C6 flow cytometer.

Affinity Chromatography of Hemocyte Extracts on CvGal1—Oyster hemocyte extracts were fractionated on a crCvGal1 column at 4 °C. The column was prepared by cross-linking crCvGal1 (10 mg/ml) to Affi-Gel 15 (Bio-Rad) according to the manufacturer's recommendations. Bound proteins were eluted in PBS containing 50 mM lactose and lyophilized. In preliminary experiments, extracts were prepared with the addition of 1% Triton X-100, and the results obtained with aqueous extracts were compared. Eluted proteins were analyzed by SDS-PAGE and visualized by Coomassie Blue stain. The most prominent bands were coded as H1–H5, excised from the gel, and subjected to proteomic analysis.

Protein Identification by Mass Spectrometry—Proteins in gel band were proteolyzed with MS grade trypsin as described previously (27). Protein identification by liquid chromatography-tandem mass spectrometry (LC-MS/MS) analysis of peptides was performed using an LTQ ion trap MS (Thermo Fisher Scientific) interfaced with an Eksigent two-dimensional nano-LC system. Peptides were fractionated by reverse phase HPLC on a 75-μm × 100-mm C18 column with a 10-μm emitter using 0–60% acetonitrile, 0.1% formic acid gradient over 90 min at 300 nl/min. Peptide sequences were identified using Mascot software to search the NCBInr 167 database with acquired raw MS data, with oxidation on methionine and carbamidomethylation on cysteine as variable modifications. Mascot search results were processed in Scaffold validate protein and peptide identifications. All samples were filtered for proteins with at least 80% confidence with peptides at 95%, and the proteins were identified at 95% or greater confidence based on the identification of at least two peptides at 95% or greater confidence.

Cloning and Identification of C. virginica β-Integrin—Based on the identification of two peptides in band H4 as matching the *Crassostrea gigas* GenBank™ sequence of β-integrin, we confirmed the presence of this transcript in the *C. virginica* hemocytes by RT-PCR following general PCR amplification and cloning procedures described elsewhere (28) (pGEM-T vector system technical manual) with degenerate oligonucleotide primers designed on two highly conserved regions of *C. gigas* β-integrin ligand binding domain (LBD1, 5′-GA(CT)CT-(N)TA(CT)TA(CT)(CT)T(N)ATGGA-3′ and 5′-TC(N)AC(A-G)AA(N)GA(N)CC(AG)AA(N)CC-3′) (28, 29). The resulting amplicon was cloned and sequenced, and the identity of the product was confirmed by nucleotide and predicted amino acid alignments of the *C. virginica* sequence with the *C. gigas* sequence.

Glycotyping of P. marinus Trophozoites with Labeled Plant Lectins—The fixed *P. marinus* (4×10^6 cells in 100 μl of HBS) was incubated with 10 μg/ml FITC-labeled ConA, SBA, GNA, UEA, WGA, or PNA for 1 h at room temperature. After three washes in HBS, the cells were suspended at 10^7 cells/ml in HBS and analyzed with an Accuri C6 flow cytometer as described above.

RESULTS

The initial characterization of CvGal1 (15) had revealed that unlike most galectins described to date, CvGal1 binds stronger to galactosamine and *N*-acetylgalactosamine than to D-galactose or *N*-acetyllactosamine, suggesting that its specificity might be directed to cell surface glycans displaying nonreducing terminal blood group oligosaccharides rather than poly-*N*-acetyllactosamines. To gain further insight into the fine specificity of CvGal1, we produced the recombinant protein and analyzed its carbohydrate-binding profile from glycan array binding studies (Core H, Consortium for Functional Glycomics).

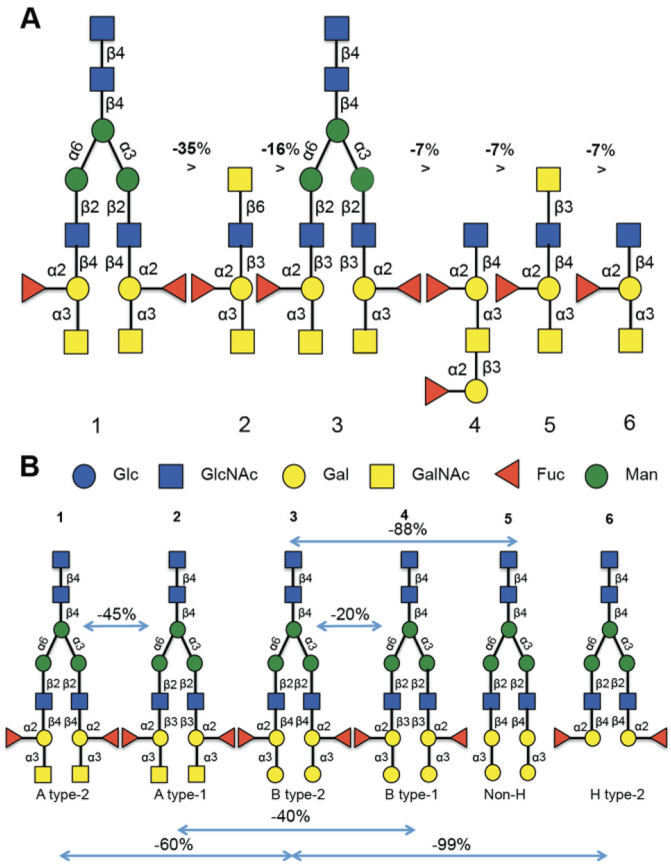

FIGURE 1. **Analysis of the specificity of CvGal1 for ABH blood group oligosaccharides.** *A*, six best glycans ranked by their affinity for CvGal1. The glycan array analysis of CvGal1 was carried out at concentrations of 2, 10, 50, and 150 μg/ml, and those oligosaccharides showing dose-dependent binding were selected for further analysis. *B*, relationship between relative fluorescent unit signals of a series of structurally related glycans recognized by rCvGal1 (10 μg/ml) in the microarray to illustrate the effect of glycosyl groups to the core galactoside on the CvGal1 affinity. The negative percentages are the evaluation of the % change in the fluorescent signal ($(F_j - F_i)/F_i \times 100\%$). The relative fluorescent unit values for the oligosaccharides 1–6 illustrated in *A* are as follows (glycan array code number is in *parentheses*): *1* (367), 20,893 ± 1382; *2* (499), 13,410 ± 711; *3* (370), 11,130 ± 794; *4* (387), 10,689 ± 350; *5* (411), 9785 ± 508; *6* (84), 9358 ± 328. The complete relative fluorescent unit dataset used for this analysis can be accessed at the website for Core H of the Consortium for Functional Glycomics.

Glycan Array Analysis—Analysis of the glycan array binding profile of rCvGal1 at different protein concentrations (2, 10, 50, and 150 μg/ml) revealed that CvGal1 recognizes with high affinity carbohydrates containing nonreducing terminal GalNAc, thereby confirming our previous results from binding-inhibition studies (15). The strongest binder in the glycan array was the complex bi-antennary GalNAcα1–3(Fucα1–2)-Galβ1–4GlcNAcβ1–2Manα1–6[GalNAcα1–3(Fucα1–2)-Galβ1–4GlcNAcβ1–2Manα1–3]Manβ1–4GlcNAcβ1–4GlcNAcβ (Fig. 1, *A1* and *B1*), followed by GalNAcα1–3(Fucα1–2)-Galβ1–3GlcNAcβ1–2Manα1–6[GalNAcα1–3(Fucα1–2)-

Galβ1–3GlcNAcβ1–2Manα1–3]Manβ1–4GlcNAcβ1–4-(Fucα1–6)GlcNAcβ (Fig. 1*B2*). This suggested that the anomeric linkage β1–4 or β1–3 of the subterminal Gal to the GlcNAc affects the binding and that CvGal1 prefers type 2 backbone structures Galβ1–4GlcNAc in *N*-acetyllactosamine, typical of most galectins described to date, and shows weaker binding to type 1 backbones Galβ1–3GlcNAc. In addition, the Fucα1–2 bound to the subterminal Gal further strengthens the binding. However, the lack of an *N*-acetyl modification on the nonreducing terminal moiety (Gal instead of GalNAc) such as in Galα1–3(Fucα1–2)Galβ1–4GlcNAcβ and Galα1–3(Fucα1–2)-Galβ1–3GlcNAcβ negatively affects rCvGal1 binding, suggesting that interactions are established between the rCvGal1 protein and the *N*-acetyl substitution of GalNAc. Thus, rCvGal1 recognizes with high specificity array elements displaying blood group A type 2 tetrasaccharides followed by the type 1 structures and, with less affinity, similar patterns of B tetrasaccharides (Fig. 1*B*), thereby displaying a clear preference for blood group A over blood group B. In contrast, substitutions in position 1 of the nonreducing terminal GalNAc ring negatively affect rCvGal1 binding but do not abolish it. For example, monosaccharide substitutions (such as terminal galactose, as in Galβ1–3GalNAcα1–3(Fucα1–2)Galβ1–4Glcβ or Galβ1–4GalNAcα1–3(Fucα1–2)Galβ1–4Glcβ) and disaccharide substitutions (such as Fucα1–2Galβ1–3 in Fucα1–2-Galβ1–3GalNAcα1–3(Fucα1–2)Galβ1–4GlcNAcβ) to the terminal GalNAc moderately affect CvGal1 binding, suggesting that these can interfere but not completely disrupt the interactions between the protein and the GalNAc moiety. Further glycosylation at the reducing end of the core glycoside has no further effect on binding as these regions are outside the binding pocket of the lectin.

TABLE 1

Pairwise percentage identity in the modeling alignment of Fig. 2

The table value at row i, column j, is the percentage of the sequence j that matches sequence I.

Galectin	*Ba*Gal1 chain A	*Cv*Gal1 Chain A	*Cv*Gal1 Chain B	*Cv*Gal1 Chain C	*Cv*Gal1 Chain D
***Ba*Gal1**					
Chain A	100.0	18.6	22.8	18.8	22.8
***Cv*Gal1**					
Chain A	20.1	100.0	33.1	32.6	37.5
Chain B	23.1	31.0	100.0	31.2	30.9
Chain C	19.4	31.0	31.6	100.0	35.3
Chain D	23.1	35.2	30.9	34.8	100.0

Comparative Modeling of the CvGal1 CRDs—We modeled the four CRDs of CvGal1 (A, amino acids 1–145; B, amino acids 146–281; C, amino acids 282–419; and D, amino acids 420–555) using as template the structure of the galectin-1 from the South American toad *B. arenarum* (BaGal1; PDB code 1GAN) (24). BaGal1 and the four CRDs of CvGal1 have pairwise sequence identities ranging from 18.6 (Table 1, row 1, column 2) to 22.8% (Table 1, row 1, column 5). Alignment of the CRDs

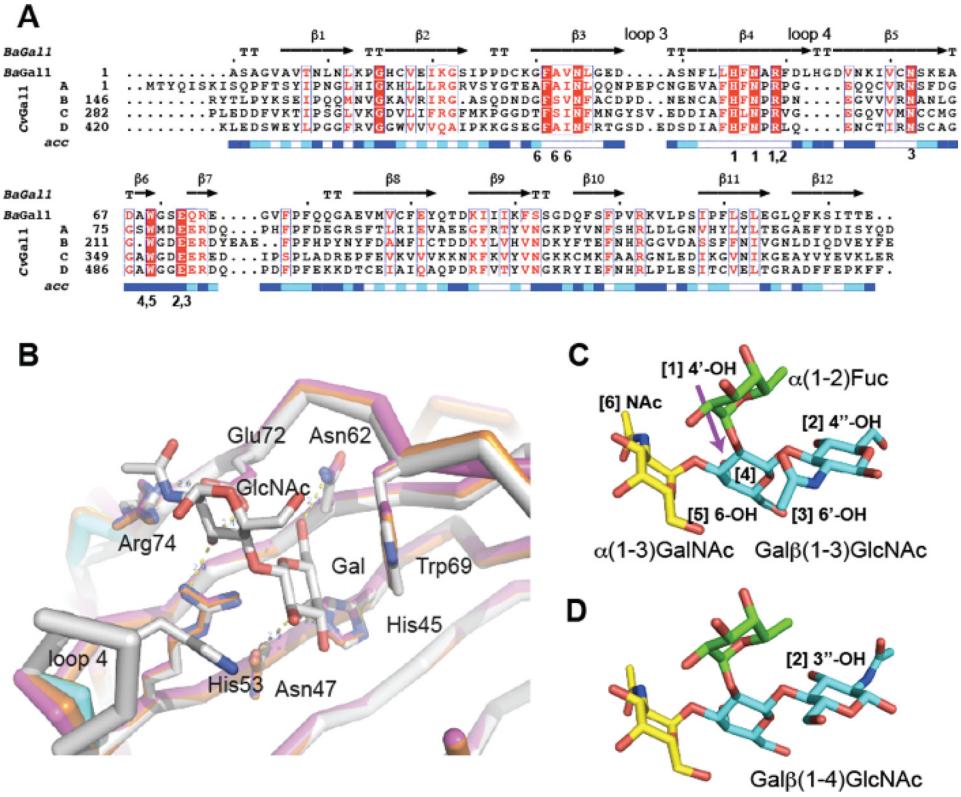

FIGURE 2. **Sequence analysis of CvGal1 and the modeling template BaGal1 and interactions of BaGal1 with *N*-acetyllactosamine and blood group A oligosaccharides.** *A,* sequence alignment of the template, *B. arenarum* galectin-1 (BaGal1; PDB code 1GAN (24)), and the four CRDs (peptides A, B, C, and D) of CvGal1 is shown. The secondary structure elements of the template are indicated above the corresponding residues. Identical residues are *white with red background*; regions scoring higher than 70% using a Risler's similarity scoring-matrix (60) are *boxed* with *red letters*. The figure was made using ESPript. The *numbers* below the residues indicate the recognition of a particular carbohydrate epitope of *C* and *D*. *B,* in the overlay between the modeled CvGal1 CRDs and BaGal1, a bound *N*-acetyllactosamine is shown. Loop 4 of the CvGal1 CRDs is shorter than the loop 4 of BaGal1. See also supplemental Fig. S1. *C,* recognition of A type 1 (Galβ(1–3)GlcNAc) oligosaccharide. *D,* recognition of A type 2 (Galβ(1–4)GlcNAc) oligosaccharide. Carbohydrate epitopes are labeled with *numbers in parentheses* that are associated with residues in *A* that recognize them.

with BaGal1 (Fig. 2*A*) shows that most residues that participate in the recognition of the Galβ(1–4)GlcNAc in BaGal1 are conserved in all CvGal1 CRDs (Fig. 2*B*). These conserved residues generate interactions of the binding site with four epitopes of the galactoside moieties shown in Fig. 2, *C* and *D*, as follows: 1) (Arg-49, His-45, Asn-47)-4-OH of Gal; 2) (Arg-49, Glu-72) (3-OH in core 1, or 4-OH in core 2 galactosides) of GlcNAc; 3) (Asn-62, Glu-72)-5-OH of Gal; and 4) Trp-69-ring of Gal, due to which, their relative position in the models were strictly preserved (Fig. 2*B*).

Two differences in the secondary structure elements of CvGal1 CRDs with respect to the template, also to known mammalian galectin-1, are evident from the inspection of the modeling alignment as follows: a longer sequence between strands 3 and 4 (loop 3) and a shorter loop between strands 4 and 5 (loop 4) (Fig. 2*A*). The CvGal1 model predicts relatively minor differences among the four CRDs, mostly concentrated in loops 3–5 (supplemental Fig. S1). Of these, only loop 4 (in BaGal1) participates in the recognition of the galactose moiety, whereby a histidine residue (His-53 in BaGal1) makes an apolar contact with the C2 and O2 atoms of the Gal moiety of the core 2 galactoside (Fig. 2*B*). The absence of loop 4 in the CRDs of CvGal1 removes this histidine residue that in other galectins-1 participates in carbohydrate recognition (Fig. 2*A*).

Modeling the Recognition of Blood Group A Type 1 and 2 Oligosaccharides—To visualize the recognition of these blood group antigens (Fig. 2, *C* and *D*) by CvGal1, one of these carbohydrates was docked to the model of the first CvGal1 CRD, using the *N*-acetyllactosamine bound to BaGal1 (PDB code 1GAN) as guide to dock the same moiety of the tetrasaccharide to the CvGal1 CRDs. Fig. 3*A* shows the type 2 blood group A oligosaccharide (A2) bound to the first CRD of CvGal1 as representative of the recognition of A and B blood group antigens by all the CvGal1 CRDs. The 2′-fucosyl moiety of the tetrasaccharide, which is a feature common to both the A and B blood group tetrasaccharides, is accommodated in the space generated by the shortening of loop 4 (Fig. 2*B*). Its 6-methyl group lies on top of the arginine residue that coordinates the equatorial OH group of the core galactoside's second moiety (Fig. 3*A*). The conserved glutamate in CvGal1 CRDs at the end of the short loop 4 is holding the arginine that coordinates the 3-OH group (Fig. 3*A*). No direct interaction of a protein polar group with fucose hydroxyls is expected, although particular CRD residues such as Glu-37 in the A CRD, Asn-199 in the B CRD, and Glu-449 and Glu-474 in the D CRD are at distances that could form water-mediated bridges between the protein and the fucose 4-OH group (distances between 4.3 and 5.4 Å). A similar coordination of an A2 tetrasaccharide was observed in its complex with the fungal galectin CGL2[4] (Fig. 3*B*) (40).

The α(1–3)-linked Gal(NAc) moiety of the A and B blood group tetrasaccharides is recognized by the 5-NH of the conserved tryptophan (Trp-77 in the first CRD of CvGal1; Fig. 3*A*). This NH group provides an H-bond to the Gal(NAc) 6-hydroxymethyl group in a *gt* conformation (O6 gauge to O5 and *trans* to C4; interaction *5* in Fig. 2, *C* and *D*). The hydroxyls

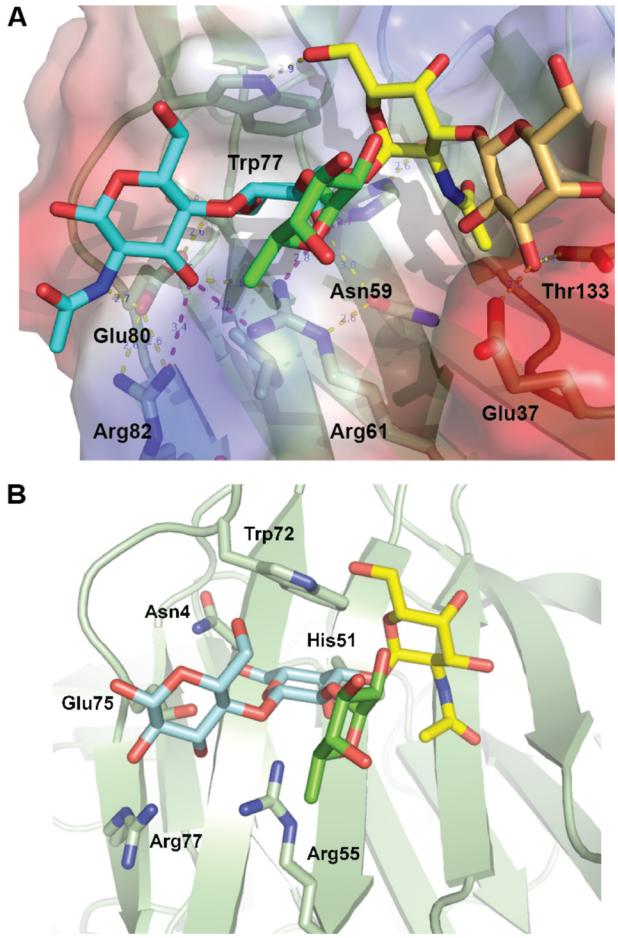

FIGURE 3. **Recognition of blood group A type 2 oligosaccharides by CvGal1 and CGL2.** *A,* A2 blood antigen docked at the binding pocket of the CvGal1 model of the first CRD, using the observed common *N*-acetyllactosamine disaccharide bound to the template. CvGal1-binding site is shown as semi-transparent solvent-accessible surface colored by its vacuum electrostatic potential (positive in *blue* to negative in *red*). The schematic model of the protein is visible across the surface showing the interacting residues in a *stick* representation. H-bonds recognizing hydroxyl groups of the A2 antigen are displayed as *dashed lines* with their distances (in Å) between heavy atoms indicated. *B,* A2 bound to CGL2; PDB code 1UFL. The carbon atoms of the *N*-acetyllactosamine moiety are colored in *cyan*, the α(1–3)GalNAc in *yellow*, and α(1,2)-Fuc in *green*. All nitrogen atoms are colored in *blue*. See also supplemental Fig. S2.

at 3 and 4 positions of the α3-linked Gal(NAc) moiety are not directly recognized by protein groups. A hydrophobic pocket at the external side of the strand β3 (amino acids 30–38 in Fig. 2*A*) recognizes the methyl of the 2-NAc group of α3-linked GalNAc of A1/2 antigens (interaction *6* of Fig. 2, *C* and *D*). Additional carbohydrate moieties can be accommodated at the nonreducing end, and arguably they may form H-bonds with polar residues in strands β11 and β4.

ELISA and SPR Analysis of CvGal1 Binding to Blood Group-related Mono- and Oligosaccharides—To experimentally validate the models described above, we first comparatively assessed by ELISA the binding of rCvGal1 and anti-A monoclonal antibodies to neoglycoproteins displaying either a monosaccharide (GalNAc), a blood group A trisaccharide (GalNAcα3-(Fucα2)Gal), or a type 2 tetrasaccharide (GalNAcα3(Fucα2)-Galβ3GlcNAc) conjugated to BSA. The results were striking because the anti-A antibody bound equally well to the blood

[4] The assignment of the *N*-acetyl conformer deposited in the PDB seems to be incorrect (the methyl of the *N*-acetyl group coordinates a water molecule).

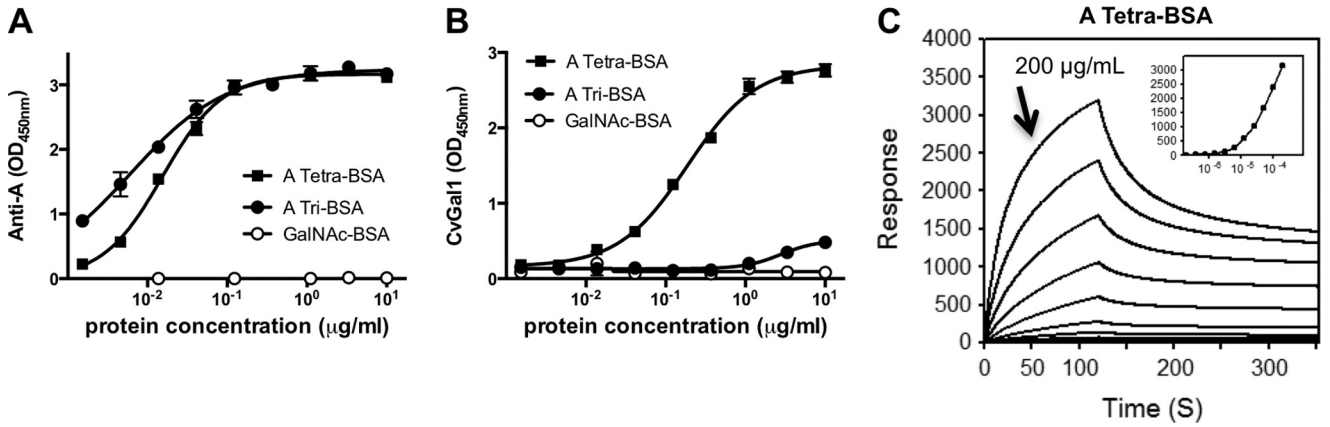

FIGURE 4. **Binding of rCvGal1 and anti-A monoclonal antibodies to neoglycoproteins.** *A* and *B*, ELISA: blood group A tetrasaccharide-BSA (*tetra-BSA*), blood group A trisaccharide-BSA (*tri-BSA*), or *N*-acetylgalactosamine-BSA (*GalNAc-BSA*) were delivered at the concentrations indicated (serial dilution starting from 10 μg/ml, 100 μl/well) into 96-well plates and incubated overnight. After blocking and washing the plates, the binding of mouse monoclonal anti-A antibodies (1:2000) (*A*) and CvGal1 (0.2 μg/ml) (*B*) was assessed. *C*, SPR measurements: blood group A tetrasaccharide-BSA, blood group A trisaccharide-BSA, or GalNAc-BSA were immobilized on CM5 chips, and binding of rCvGal1 was assessed by SPR flowing through rCvGal1 in 2-fold serial dilutions (starting from 200 μg/ml) as analyte. Sensorgrams and the 1:1 affinity curve (*inset*) for the binding of rCvGal1 onto blood group A tetrasaccharide-BSA are shown. Negligible responses were observed on sensorgrams for the other two neoglycoproteins, blood group A trisaccharide-BSA and GalNAc-BSA (data not shown).

group A tri- and tetrasaccharides and showed negligible binding to GalNAc-BSA (Fig. 4*A*); CvGal1 only recognized the blood group A tetrasaccharide (Fig. 4*B*). The quantitative analysis by SPR revealed that rCvGal1 binds to the neoglycoprotein displaying blood group A type 2 tetrasaccharide with a K_D value of 1.5 μM (Fig. 4*C*), although no apparent binding to either blood group A trisaccharide-BSA or the tested monosaccharides (GalNAc, Gal, and GlcNAc) conjugated to BSA was observed under the same binding conditions used for assessing the binding of blood group A type 2 tetrasaccharide (results not shown).

Specificity of CvGal1 for Glycoproteins—We evaluated by a solid phase assay the inhibition of the binding of CvGal1 to asialofetuin by glycoproteins that display some of the oligosaccharides identified as CvGal1 ligands in the glycan array (Fig. 5*A*). These include glycoproteins that display abundant blood group A oligosaccharides, like PSM (30), and the desialylated forms of PSM and fetuin that exhibit nonreducing terminal galactose (31). Asialo-PSM (IC_{50} = 0.003–0.007 μg/ml) and PSM (IC_{50} = 0.012–0.028 μg/ml) behaved as the strongest inhibitors, at least >40-fold better than any other glycoprotein tested. These were followed by BSM (IC_{50}, 0.580 to 1.074 μg/ml), and OSM (IC_{50}, 4.54 to 11.02 μg/ml) (Table 2). The strongest inhibition by asialo-PSM suggests that in addition to GalNAc, CvGal1 also binds to unmasked Gal moieties on the desialylated glycoprotein (Fig. 5*A*). In reciprocal experiments, in which the binding of CvGal1 to PSM bound to the plate was tested for inhibition by glycoproteins, no significant inhibition was observed at concentrations reaching up to 1 mg/ml (data not shown).

To investigate whether the binding of CvGal1 to PSM was due to interactions between the galectin and the carbohydrate component of PSM, and to find out if the oligosaccharides recognized were either part of *N*-linked or *O*-linked glycans or both, we tested the binding of CvGal1 to PSM that had been treated with PNGase F and *O*-glycosidase. The results indicated that treatment of PSM with PNGase F reduced the binding in about 50%, whereas treatment with *O*-glycosidase reduced the binding in about 35%, suggesting that CvGal1 binds to both N- and *O*-linked carbohydrate components of PSM (Fig. 5*B*).

We subsequently assessed by SPR the binding kinetics of CvGal1 to the glycoproteins identified above as CvGal1 ligands, such as PSM and asialofetuin, and other glycoproteins. The results showed that in agreement with the binding-inhibition studies, PSM behaved as the strongest binding ligand with a K_D value of 4.7 nM (Fig. 5*C*), although for asialofetuin, the binding of CvGal1 was significantly weaker ($K_D \geq 300$ μM) (Fig. 5*D*).

Binding Specificity of CvGal1 for Oyster Hemocyte Glycans—To examine if the binding of CvGal1 to mammalian glycoproteins could be translated into binding to biologically relevant glycans, namely those on the surface of the oyster hemocytes and those on the surface of *P. marinus* trophozoites, we first assessed by a solid phase assay the binding of CvGal1 to hemocyte extracts, and the relative strength of the binding by binding-inhibition studies that included the glycoproteins previously characterized as ligands (asialofetuin and PSM) and the hemocyte extract itself. The results showed that CvGal1 bound to the hemocyte extracts in a dose-dependent manner. Furthermore, despite PSM being such an effective ligand for CvGal1, the hemocyte extract behaved as the strongest ligand (Fig. 6*A*). This suggests that the natural self-carbohydrates on the surface of the hemocyte are the preferred ligands for CvGal1.

To evaluate the contributions of *N*-linked or *O*-linked glycans or both to CvGal1 binding to hemocyte extracts, we tested the binding of rCvGal1 to hemocyte extracts that had been treated with PNGase F and *O*-glycosidase, with the untreated extract as control. The binding to both the enzyme-treated extracts was similarly reduced approximately in >60% (Fig. 6*B*), suggesting that both types of linked oligosaccharides are recognized by CvGal1.

Given the binding preference of CvGal1 for blood group A oligosaccharides and the *N*-glycomic data indicating their presence in oyster plasma and hemocyte glycoproteins (61), we assessed the possibility that the carbohydrate moieties recognized by CvGal1 on the hemocyte extracts are actually, at least in part, blood group A oligosaccharides. We tested the binding

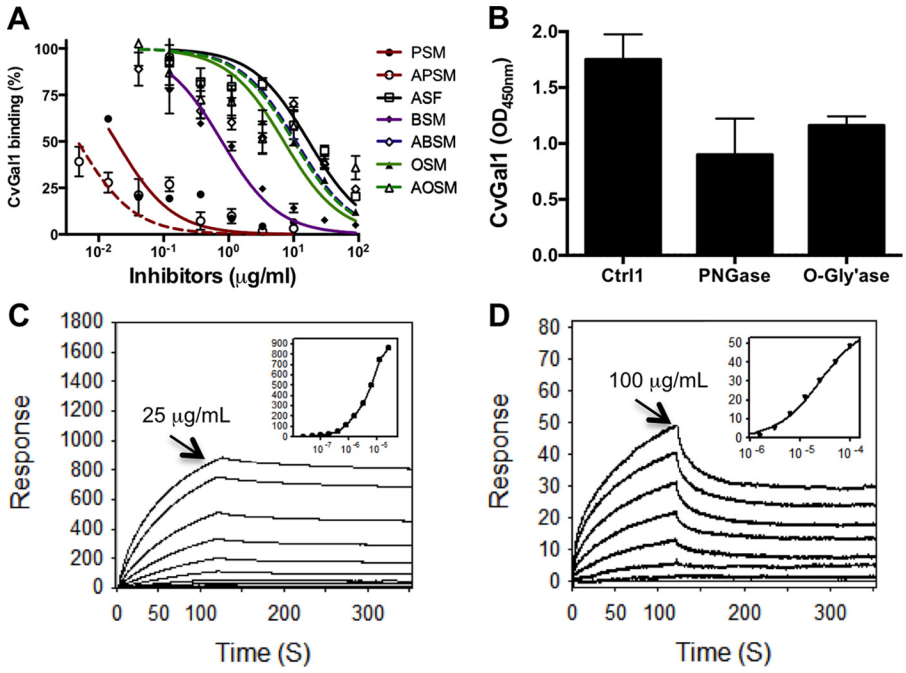

FIGURE 5. **Binding of rCvGal1 to natural glycoproteins.** *A,* binding of rCvGal1 to asialofetuin (20 μg/ml) in the presence of serial dilution of PSM, asialo-PSM (*APSM*), asialofetuin (*ASF*), BSM, asialo-BSM (*ABSM*), OSM, or asialo-OSM (*AOSM*) was measured in solid-based binding assay. Data show relative binding in triplicate with standard error. IC_{50} values (50% inhibition concentrations) were calculated (Table 2). *B,* binding of rCvGal1 to untreated (*Ctrl*), or PNGase F-treated, or *O*-glycosidase (*O-Gly'ase*)-treated PSM-coated plates were measured. *C,* SPR was measured with immobilized PSM and rCvGal1 as analyte as for Fig. 4. SPR sensorgram was shown with *inset* as 1:1 steady state fitting curve. *D,* SPR was measured with immobilized asialofetuin and rCvGal1 as analyte. The surface plasmon resonance sensorgrams were recorded with 2-fold serial dilutions starting at the highest concentration labeled. SPR sensorgram was shown with *inset* as 1:1 steady state fitting curve.

TABLE 2
Inhibition of CvGal1 binding onto asialofetuin by glycoproteins

Inhibitor	IC_{50} (95% interval)
	μg/ml
Asialofetuin	10.87–26.82
PSM	0.0123–0.0284
Asialo-PSM	0.00304–0.00748
BSM	0.580–1.074
Asialo-BSM	5.54–21.4
OSM	4.54–11.02
Asialo-OSM	5.09–19.9

of anti-A monoclonal antibodies to the hemocyte extracts, with and without pretreatment with glycosidases. These included *N*-acetylgalactosaminidase, fucosidase, and galactosidase as individual treatments or combined subsequent treatments of the same extract. The results clearly showed that the anti-A monoclonal antibodies strongly bind to the hemocyte extracts in a glycan-specific manner. α-*N*-Acetylgalactosaminidase treatment of the hemocyte extract reduced rCvGal1 binding in about 70% and fucosidase in 50%, whereas β1,3-galactosidase had no significant effect. The triple treatment reduced the binding to a level similar to the α-*N*-acetylgalactosaminidase alone (Fig. 6*C*).

We then addressed the question if the A oligosaccharides recognized by the anti-A monoclonal antibodies are the same moieties recognized by CvGal1 both in PSM and in the hemocyte extracts. For this we conducted assays aimed at assessing the competitive blocking of CvGal1 binding to PSM and hemocyte extracts by anti-A and anti-B monoclonal antibodies. Pretreatment of PSM with anti-A reduced the CvGal1 binding in at least 60%, whereas anti-B had no effect (Fig. 6*D*). A similar experiment on hemocyte extract revealed that only anti-A significantly reduced CvGal1 binding (by about 40%), suggesting that the specificity of CvGal1 for A oligosaccharides overlaps with the anti-A antibodies (Fig. 6*D*).

Binding Specificity of CvGal1 to Oyster Circulating Hemocytes—To find out if our observations on the binding of CvGal1 to hemocyte extracts could be extended to intact hemocytes obtained from circulating hemolymph, we first examined the binding of CvGal1 to fixed, nonpermeabilized hemocytes by flow cytometry, and its inhibition by PSM and asialofetuin, using BSA as control. The CvGal1 strongly bound to the surface of the hemocytes, and the presence of PSM (300 μg/ml) virtually abolished CvGal1 binding, whereas ASF at 1 mg/ml only reduced binding in about 10%, and BSA had no inhibitory effect (Fig. 7*A*). A dose-response binding-inhibition study with PSM revealed that although 30 μg/ml PSM inhibited binding in about 30%, a 10-fold increase of the glycoprotein concentration resulted in 100% inhibition of CvGal1 binding (Fig. 7*B*).

As monoclonal anti-A antibodies recognize blood group A moieties on hemocyte extracts, we investigated whether these glycans are exposed on the hemocyte surface and may represent the hemocyte ligands recognized by CvGal1 observed in our prior study (15). For this, we carried out a competitive binding-inhibition study with anti-A monoclonal antibodies and CvGal1 similar to those carried out with the hemocyte extracts. The results suggest that the moieties recognized on the hemocyte surface by CvGal1 are the blood group A oligosaccharides also recognized by the anti-A-specific antibodies. In contrast to the strong binding of anti-A antibodies (Fig. 7*C*), the anti-B antibodies showed no binding to the intact hemocytes (results

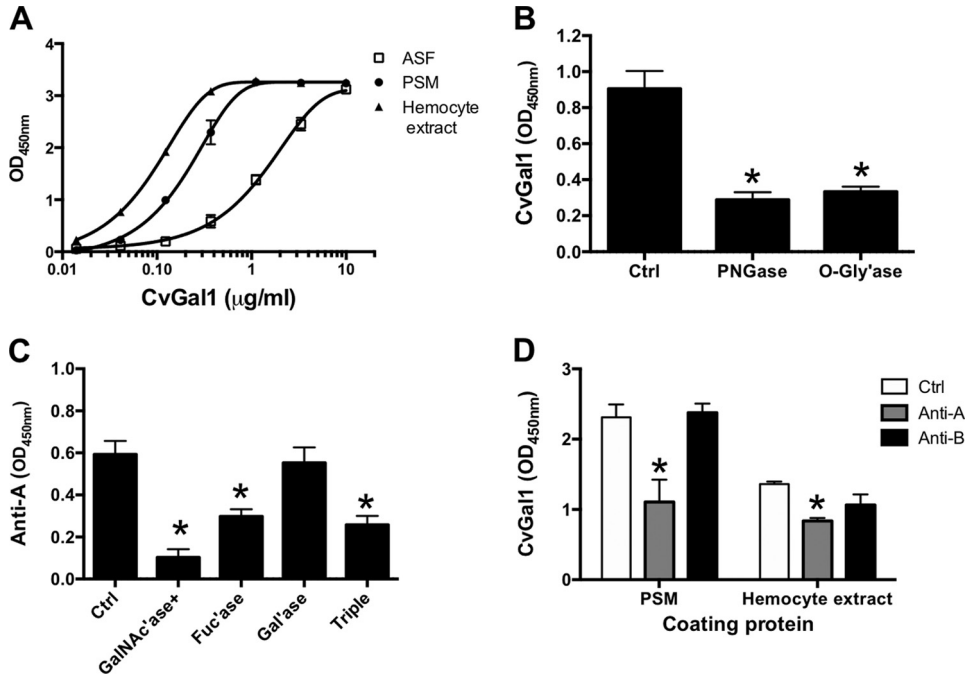

FIGURE 6. **Binding of rCvGal1 to hemocyte extract.** *A,* binding of rCvGal1 (serial dilutions 1:3) to ASF (20 μg/ml), PSM (10 μg/ml), or hemocyte extract (10 μg/ml)-coated plates was measured. *B,* binding of rCvGal1 to untreated (*Ctrl*), or PNGase F-treated, or *O*-glycosidase (*O-Gly'ase*)-treated PSM-coated plate was measured. * indicates significant difference ($p < 0.05$) from control (*Ctrl*). *C,* binding of anti-A monoclonal antibody to untreated (*Ctrl*), α-*N*-acetylgalactosaminidase-treated (*GalNAc'ase*), α-L-fucosidase-treated (*Fuc'ase*), β1,3-galactosidase-treated (*Gal'ase*), or three enzyme subsequent treatments (triple) of hemocyte extract (0.5 μg/ml)-coated plates were measured. *D,* binding of rCvGal1 (0.5 μg/ml) to PSM (0.5 μg/ml) or hemocyte extract (0.5 μg/ml)-coated plates in buffer (*Ctrl*) or in the presence of anti-blood group A (*anti-A*) or group B (*anti-B*) antibody were measured. Data show mean optical density at 450 nm in triplicates with standard deviation. * indicates significant difference ($p < 0.05$) from control (*Ctrl*).

not shown). Similarly to the solid phase assay, reciprocal partial inhibition of binding of anti-A monoclonal antibodies (Fig. 7*D*) and rCvGal1 (Fig. 7*E*) was observed, whereas the anti-B antibodies showed no inhibition on the binding to the intact hemocytes (data not shown). To examine the specificity of the binding of both CvGal1 and anti-A monoclonal antibodies to the hemocyte cell surface, we assessed the effect of enzymatic GalNAc removal from the cell surface on both galectin and antibody binding. Pretreatment of the hemocytes with α-*N*-acetylgalactosaminidase reduced the CvGal1 binding virtually to the control levels (Fig. 8*A*), suggesting that the presence of nonreducing terminal αGalNAc is critical for CvGal1 binding onto the hemocyte surface. Although the binding of anti-A antibodies was also significantly reduced (>40%) (Fig. 8*B*), the residual binding suggest that the high affinity monoclonal antibodies can still bind to remaining GalNAc residues, which are not bound by CvGal1. Consistent results were obtained by Western blotting (61).

Isolation and Identification of CvGal1 Ligands from Oyster Hemocytes—The isolation and identification of CvGal1 ligands from oyster hemocytes was carried out by affinity chromatography using an crCvGal1-Affi-Gel 15 column with subsequent SDS-PAGE. Multiple bands were visible by Coomassie Blue stain (supplemental Fig. S3). The five most prominent bands, designated as H1 to H5 (30–125 kDa), were excised from the gel and subjected to proteomic analysis. The mass spectrometry results revealed the presence of multiple peptides that matched β-integrin, dominin, GAPDH, and HSP70 in the bands of the expected electrophoretic mobilities as the proteins of interest (supplemental Fig. S4). For some of the above proteins, such as β-integrin and dominin, additional peptides were identified in bands other than those indicated in supplemental Fig. S3. The identification of β-integrin in eastern oyster (*C. virginica*) hemocytes was confirmed by cloning with primers designed on the Asian oyster (*C. gigas*) nucleotide sequence (supplemental Fig. S5).

Binding of rCvGal1 and Plant Lectins to P. marinus Trophozoites—Given the strong binding of CvGal1 to *P. marinus* trophozoites, we had observed in our previous study (15), we examined the possibility that CvGal1 recognized blood group A oligosaccharides on the parasite surface as well. For this, we first characterized by flow cytometry the binding of CvGal1 and its inhibition by PSM. Similarly to what we observed for the intact hemocytes, CvGal1 bound strongly to the trophozoites (Fig. 9*A*), and this binding could be inhibited by PSM in a dose-dependent manner (Fig. 9*B*). However, no binding of the anti-A or anti-B monoclonal antibodies to the *P. marinus* trophozoites was observed (Fig. 9*C*), indicating that neither blood group A nor B oligosaccharides are present on the parasite surface and that CvGal1 recognizes GalNAc or related ligands displayed on different carbohydrate moieties.

To investigate the possible CvGal1 ligands on the surface of *P. marinus* trophozoites, we conducted a glycotyping analysis of the parasite surface with labeled plant lectins (Fig. 9*D*). The study revealed strong binding of ConA (αMan, GlcNAc, and αGlc), SBA (α,βGalNAc and α,βGal), GNA (α1–3 and α1–6 high mannose oligosaccharides), WGA (Neu5Ac or β4-linked terminal HexNAc), and PNA (Galβ1–3GalNAcα), but no binding was observed with UEA (Fucα1–2Gal), suggesting the absence of exposed α-linked L-fucose residues, which was con-

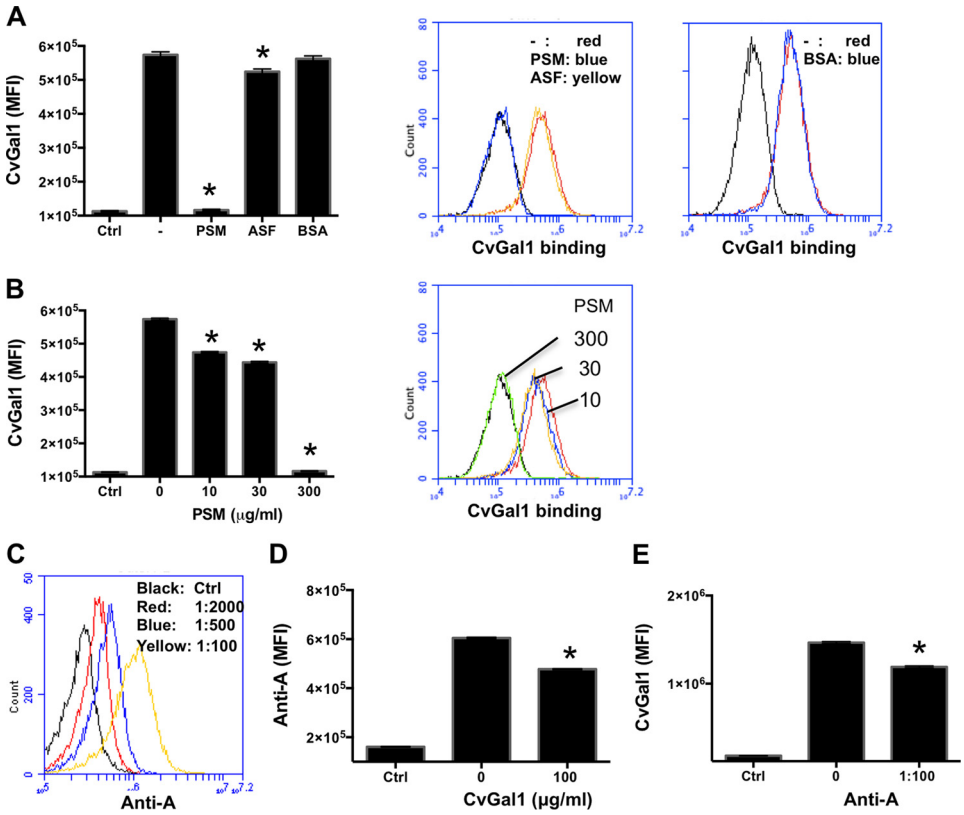

FIGURE 7. **Binding of rCvGal1 to whole hemocytes.** *A,* binding of rCvGal1 (100 μg/ml) to hemocytes in the presence of PSM (300 μg/ml), ASF (1 mg/ml), or BSA (1 mg/ml). * indicates significant different ($p < 0.05$) from sample without inhibitor (−). *B,* binding of rCvGal1 (100 μg/ml) to hemocytes in the presence of PSM (0–300 μg/ml). Sample without exogenous rCvGal1 and inhibitor was shown (*Ctrl*). * indicates significant difference ($p < 0.05$) from sample without inhibitor (*0*). *C,* fixed hemocytes were stained with dilutions of anti-blood group A antibody (*red,* 1:2000; *blue,* 1:500; *yellow,* 1:100) or buffer only (*black*) in flow cytometry analysis. Data show histogram of each sample. *D,* fixed cells were preincubated with CvGal1 (100 μg/ml) and stained with anti-blood group A antibody. Data show mean fluorescence intensity (*MFI*) ± S.E. (left panel) of each sample. * indicates significant difference ($p < 0.05$) from sample without CvGal1 preincubation (*0*). Sample without antibody staining was shown (*Ctrl*). *E,* fixed cells were preincubated with anti-blood group A antibody (1:100), and the binding of rCvGal1 (100 μg/ml) was measured. * indicates significant difference ($p < 0.05$) from sample without antibody preincubation (*0*). Sample without rCvGal1 was shown (*Ctrl*).

sistent with results reported elsewhere in a different *P. marinus* strain (32). The strong fluorescence signals recorded for SBA and PNA binding to the *P. marinus* trophozoites are of particular interest because they reveal the presence of *N*-acetylgalactosaminyl and galactosyl moieties on the parasite surface. Although due to their anomeric linkages these moieties are not recognized by either the anti-A or anti-B monoclonal antibodies, they may still be effective ligands for CvGal1, and this could explain the strong binding of CvGal1 to the parasite surface.

DISCUSSION

Virulence mechanisms of the parasite *P. marinus* for the eastern oyster *C. virginica* have generated great interest during the past few years due to the progressive decline of native and farmed oyster populations caused by Dermo disease along the east coast of the United States, with the resulting collapse of the shellfishery and loss of integrity of the estuarine ecosystem (4, 5, 8, 9). Furthermore, analysis of the oyster *P. marinus* interactions has recently become the focus of attention as a very useful model system to gain insight into the mechanistic aspects of host recognition, entry, and intracellular survival strategies of intracellular parasites of biomedical interest, as well as host responses (15, 19). In this regard, the reciprocal recognition of host and parasite glycomes by soluble or cell-associated lectins is currently accepted as a pivotal component of the host-parasite association (33, 34).

Our initial studies on the oyster revealed a complex soluble and hemocyte-associated lectin repertoire with multiple specificities (6, 7). The most prominent lectins recognize glycoproteins displaying nonreducing terminal galactose and *N*-acetylated hexosamines (7), which were present on the surface of the *P. marinus* trophozoites (32), suggesting that these lectins might function as PRRs. One of these lectins, CvGal1, is a galectin of unique four-CRD organization that, unlike most galectins described to date, showed stronger binding to galactosamine and *N*-acetylgalactosamine than to D-galactose (15). Expression of CvGal1 is up-regulated upon infectious challenge, and the protein localizes to the cell periphery and is secreted and binds to the hemocyte glycocalyx, with the remaining CvGal1 free in the extracellular compartment. We showed that the oyster recognizes bacteria and microalgae via CvGal1, which by agglutination and cross-linking of sugars on their glycocalyx with the hemocyte surface promotes phagocytosis and processing of the recognized cells either as a defense mechanism against potential pathogens or as phytoplankton food for intracellular digestion (15). Notably, *P. marinus* trophozoites are

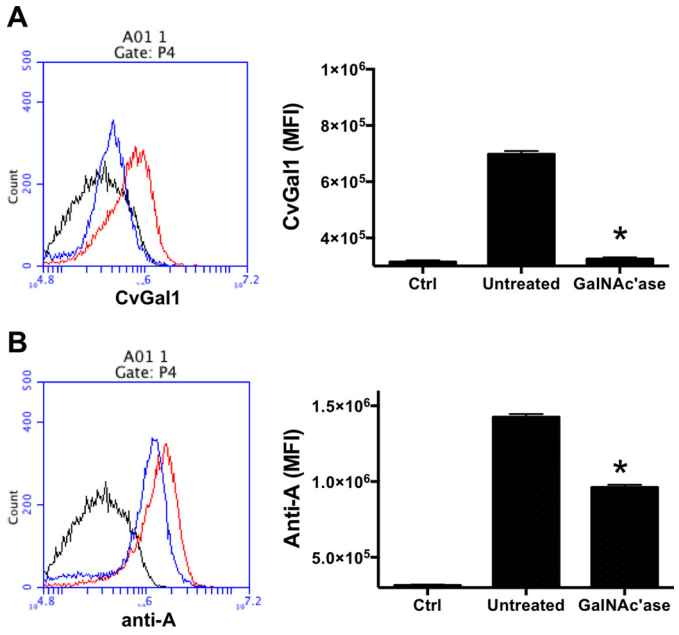

FIGURE 8. **Binding of rCvGal1 to intact and glycosidase-treated hemocytes.** Binding of rCvGal1 (*A*) or anti-blood group A antibody (*B*) to unattached hemocytes with α-*N*-acetylgalactosaminidase treatment (*GalNAc'ase*, *blue line*) or no treatment (*Untreated*, *red line*) were measured by flow cytometry. Sample without rCvGal1 or antibody staining was shown (*Ctrl*, *black line*). Data show histograms (*left panel*) and mean fluorescence intensity (*MFI*) ± S.E. (*right panel*) of each sample. * indicates significant difference ($p < 0.05$) from untreated sample.

strongly recognized by CvGal1 and subvert CvGal1 function to a parasite receptor that facilitates passive host entry by phagocytosis (15).

In this study we characterized in detail the specificity of CvGal1, and the nature of its carbohydrate ligands on the surfaces of the oyster hemocyte and the parasite *P. marinus*. Analysis of the glycan array binding profiles revealed that CvGal1 preferentially binds to ABH blood group oligosaccharides, with type 2 A tetrasaccharides as the strongest binders, followed by the type 1 structures, and with less affinity for the B tetrasaccharides. As described in the accompanying article (61), blood group A modifications of type 1 structures are found on a range of oyster glycans; thus, type 1 blood group A glycans are probably the strongest binding ligands in the biological context.

Although most galectins described to date recognize oligosaccharides exhibiting galactosyl units at the nonreducing end, particularly *N*-acetyllactosamine moieties (35), galectins from disparate taxa as fungi and mammals display specificity for ABH blood groups (36–38). Among these, the galectin CGL2 from inky cap mushroom *Coprinus cinereus* displays *in vitro* specificity for blood group A oligosaccharides (39, 40), whereas the mammalian galectins 2–4 and 8 can recognize A and B oligosaccharides in a concentration-dependent manner (36, 37). Although not specific for A oligosaccharides, some galectins can recognize nonreducing terminal GalNAc moieties in exogenous ligands, such as the human galectin-3 that binds to soluble and egg shell-associated glycans of the parasite helminth *Schistosoma mansoni* displaying GalNAcβ1–4GlcNAc (41). Furthermore, recent studies have shown that *in vivo* CGL2 actually binds the "galactosylated core fucose" glycotope (42), whereas CGL3, another galectin from *C. cinereus*, recognizes *N*-acetylhexosamines (HexNAc) such as in GlcNAc-GlcNAc or GalNAc-GlcNAc *in vitro* but not lactose (43).

The model of CvGal1 provided the structural basis for the specificity revealed by the glycan array analysis as well as ELISA and SPR data. The preference of CvGal1 for nonreducing terminal GalNAc over Gal is due to the interaction established between the protein and the *N*-acetyl side chain of GalNAc. A pocket formed at the N terminus of β3 (Fig. 2*A*; 1GAN residues 30–33) (G/A/S/T)**F**(A/S)*h***N** (where *h* stands for hydrophobic) docks the methyl group of the carbohydrate NAc moiety. Despite the taxonomic disparity and low sequence homology (supplemental Fig. S2), a similar pocket and recognition of the *N*-acetyl of GalNAc is observed in CGL2 (40). Less obvious, however, was the contribution of the fucose α(1,2) linked to the subterminal Gal to explain the preference of CvGal1 for A oligosaccharides because no direct polar interactions with protein groups are predicted with this fucosyl group. However, it is noteworthy that the shorter loop 4 makes ample room for the α(1,2)-fucosyl group and water molecules that may mediate interactions with the protein. Strikingly, the fungal galectin CGL2 shows a short loop 4 like the four CRDs of CvGal1, and CGL2 recognizes A oligosaccharides through a water-mediated interaction to the ring oxygen of the fucose (40). The α(1,3)-anomeric linkage of GalNAc to the subterminal galactose also contributes to the specificity of CvGal1. The 6-OH of the α(1,3)-linked galactose forms an H-bond with the 5-NH group of the binding site tryptophan in CvGal1 (Trp-69 of BaGal1). A similar interaction takes place between CGL2 and the α(1,3)-anomeric linkage of GalNAc to the subterminal galactose (40). The lack of binding of CvGal1 to the blood group A trisaccharide indicates that the fourth unit at the reducing end of the oligosaccharide ligand establishes key interactions with the CvGal1 extended recognition site. In many galectins, there are normally interactions with the β-galactose provided by the loop-4 histidine; however, the lack of this histidine in CvGal1 arguably weakens the recognition of core galactosides. No clear trends for CvGal1, however, are observed when an additional glycosyl is present at the lactosamine's reducing end, a consequence of the placement of the additional unit outside the galectin extended recognition site. Notably, these observations also underscored the differences in specificity between CvGal1 and the anti-A antibodies that recognized the A tetra- and trisaccharides equally well. Rather, the CvGal1 CRD is structured as those of the fungal galectins CGL2 and CGL3 and the striking similarities between CvGal1 and CGL2, despite the taxonomic disparity and low sequence homology. Similar coordination of an A2 tetrasaccharide was observed in its complex with the fungal galectin CGL2.

The strong binding of CvGal1 to PSM, relative to any other glycoprotein such as fetuin and asialofetuin, revealed that glycans that display blood group A oligosaccharides (30) behaved as the strongest ligands. The CvGal1 binding profile upon deglycosylation of PSM with PNGase F and *O*-glycosidase confirmed that the CvGal1 binding to PSM is carbohydrate-mediated and that the carbohydrate components recognized by CvGal1 are both *N*- and *O*-linked. PSM is particularly rich in oligosaccharides that display nonreducing terminal GalNAc and L-Fuc, in the form of blood group A (GalNAcα1–3-

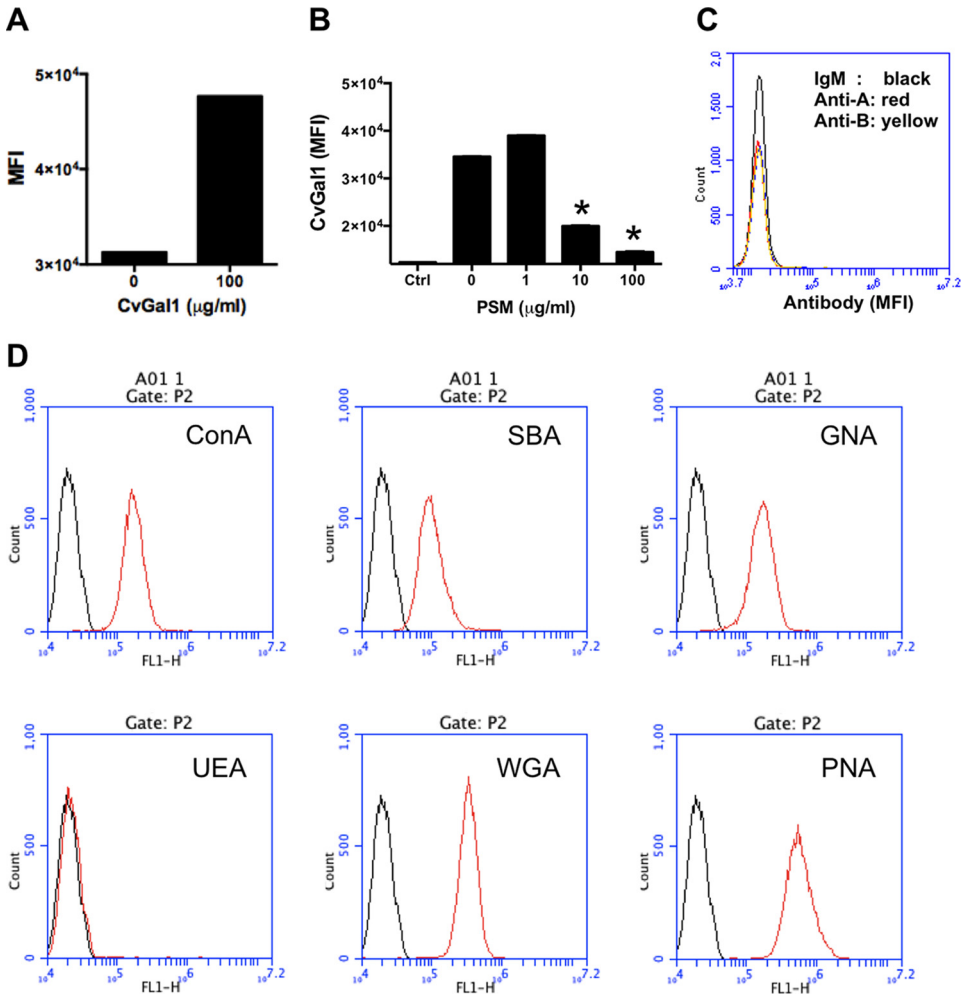

FIGURE 9. **Binding of rCvGal1 to *P. marinus* trophozoites.** *A,* binding of rCvGal1 (100 μg/ml) to *P. marinus* trophozoites was measured by flow cytometry analysis. Data show mean fluorescence intensity (*MFI*) ± S.E. of each sample. *B,* binding of rCvGal1 (100 μg/ml) to *P. marinus* trophozoites in the presence of PSM (0–100 μg/ml). * indicates significant difference ($p < 0.05$) from sample without PSM inhibition (*0*). Sample without exogenous rCvGal1 and inhibitor was shown (*Ctrl*). *C, P. marinus* trophozoites were stained with anti-blood group A antibody (*red line*), anti-blood group B antibody (*yellow line*), or control (*black line*) in flow cytometry analysis. *D, P. marinus* trophozoites were stained with fluorochrome-labeled lectins (*red lines*) or buffer alone (*black lines*) in flow cytometry analysis.

(Fucα1–2)Galβ1–4GlcNAcβ) and H (Fucα1–2Galβ1–4-GlcNAcβ) glycotopes (30), whereas fetuin is rich in sialylated *N*-acetyllactosamines (Siaα2–3Galβ1–4GlcNAcβ) (31). The significantly stronger binding of CvGal1 to asialo-forms of PSM and fetuin indicates that this galectin may also bind to subterminal residues, such as Gal, exposed by the cleavage of nonreducing terminal sialic acids. Reported Gal contents from the glycoproteins tested (fetuin, 4.1–5.5% (w/v)) and (PSM, 20–28% (total hexoses)) correlated consistently with the inhibitory capabilities of the desialylated forms, probably due to the fact that Gal is mostly in a position subterminal to sialic acid (30, 31). However, although PSM has almost 4–6 times more Gal than fetuin, the terminal GalNAc present in the PSM oligosaccharides is mostly responsible for the high inhibitory capacity of asialo-PSM relative to asialofetuin.

Multiple approaches to examine the binding of CvGal1 to the oyster hemocyte glycoproteins were consistent with those carried out with mammalian glycoproteins and revealed that the hemocyte surface ligands for CvGal1 are mostly blood group A oligosaccharides (Figs. 6–8). First, the deglycosylation of hemocyte extracts by PNGase F and *O*-glycosidase drastically reduced CvGal1 binding, thereby confirming that the CvGal1-hemocyte interactions are carbohydrate-mediated (Fig. 6*B*). Second, the effective inhibition of CvGal1 binding to hemocyte extracts by PSM and less effectively by asialofetuin strongly suggested that glycans that display blood group A glycotopes are the moieties recognized by CvGal1. Third, the inhibition of CvGal1 binding by pre-exposure of the hemocyte extracts to anti-A monoclonal antibody revealed that the two binding proteins compete for the same glycan structures, namely the blood group glycotopes (Fig. 6*D*). The drastic reduction of the monoclonal anti-A antibody binding upon the specific deglycosylation by *N*-acetylgalactosaminidase and fucosidase of the hemocyte extracts unequivocally demonstrates that αGalNAc is the main carbohydrate determinant recognized at the nonreducing end of the hemocyte oligosaccharides, although the presence of αL-fucose significantly contributes to the binding of anti-A antibodies (Fig. 6*C*). Analysis of the binding of CvGal1 to the intact oyster hemocytes demonstrates that the glycans displaying the blood group A oligosaccharides present in the hemocyte extracts are exposed on the hemocyte surface (Fig. 7*C*). CvGal1

bound to the intact hemocytes in a dose-response manner, and this could be abolished by PSM but not with asialofetuin or fetuin. Furthermore, CvGal1 and the anti-A monoclonal antibody could reciprocally compete for their hemocyte surface glycotopes (Fig. 7, *D* and *E*), and treatment of the intact hemocytes with *N*-acetylgalactosaminidase abolished CvGal1 binding (Fig. 8*A*), demonstrating unequivocally that GalNAc is the main carbohydrate determinant recognized at the nonreducing end of the oyster hemocyte surface oligosaccharides.

The presence of blood group A moieties as a potential norovirus receptor on oyster gut epithelial cells was proposed upon a norovirus outbreak resulting from oyster consumption (44, 45). Our study extends this observation to oyster hemocytes, and together with the study of Kurz *et al.* (61), it rigorously demonstrates the nature of the oligosaccharides involved. The detailed *N*-glycomic studies carried out by Kurz *et al.* (61) on plasma and hemocyte glycoproteins, as well as selected glycoproteins isolated on a CvGal1 column, identified a complex and diversified set of core and antennal modifications in the hemocyte glycans, with blood group A oligosaccharide components that provided the structural basis for our observations. A proportion of hemocyte glycans displayed core α1,3-fucosylation as well as an unusual core hexose absent from those present in plasma. Furthermore, the study demonstrated the presence of H-type α1,2-fucosylation, which together with the finding of terminal GalNAc on *N*- and *O*-glycans revealed the presence of blood group A-like moieties in the oyster hemocytes. The identified hemocyte glycans were very frequently methylated and sulfated (61), with the latter potentially conferring a significant negative charge to the hemocyte glycocalyx. Interestingly, our modeling of CvGal1 revealed that methyl and sulfate groups at 4-OH and 6-OH of the GalNAcα(1–3) are allowed, but no direct recognition by a protein group is expected; however, as these structures were absent from the array, the significance of these modifications for binding is unclear.

The results of the glycomic analysis are supported by genomic information that confirms that oysters probably express the α1,2-fucosyltransferase that can transfer L-Fuc to Gal (46). In addition, the stronger inhibition of CvGal1 binding to asialofetuin by the hemocyte extracts over any of the mammalian glycoproteins, including the best inhibitors PSM and asialo-PSM, strongly suggests that the oyster's endogenous ligands on the surface of the hemocyte display the A oligosaccharide in a scaffold or particular geometry that is preferred by CvGal1 over the mammalian glycoproteins tested. This supports the notion that the four tandemly arrayed CRDs of CvGal1 are displayed in a spatial geometry that has been evolved to recognize with high avidity a multivalent display of glycan ligands. On the oyster hemocyte surface, these self ligands would be of a defined type and density that are functionally relevant to innate immunity and feeding functions, including cell activation, phagocytosis, and intracellular digestion (15).

The proteomic analysis of the glycoproteins from hemocyte extracts that were specifically bound by CvGal1 revealed potential hemocyte surface ligands for CvGal1 that are of great interest. These were of two main types as follows: soluble glycoproteins such as dominin, and transmembrane glycoproteins such as β-integrin. Dominin is of particular interest because it is a major plasma protein in the oyster hemolymph that exhibits a Cu,Zn-superoxide-like domain and has high similarity to cavortin, an iron-binding protein from the Pacific oyster (*C. gigas*) (47). We have characterized the role of iron for *P. marinus* virulence (48–50) and intracellular survival in oyster hemocytes (51) and identified the iron uptake mechanisms via the Nramp transporter (52, 53), responsible for a "tug of war" for available iron between the parasite and its oyster host (54). A rigorous glycomic analysis of dominin associated with hemocytes and from plasma revealed that it also displays biantennary glycans carrying blood group A moieties (61), thus opening the possibility that CvGal1 cross-links dominin to the hemocyte surface as a mechanism to sequester plasma iron into the intracellular pools, a defense mechanism against infectious challenge that has been conserved from invertebrates to mammals (55). Similarly, parasite *P. marinus* could have evolved not only to subvert the role of CvGal1 to enter the hemocyte but also to bind dominin via CvGal1 and access the iron stores in both the extra- and intracellular environments.

The finding that β-integrin is among the CvGal1 ligands on the hemocyte surface is intriguing, because in mammals this transmembrane signaling glycoprotein is not only a recognized galectin ligand (56) but is also pivotal in cell activation processes (57, 58). The binding of galectins to the cell surface can form multivalent complexes (lattices) with cell surface glycoconjugate, and deliver a variety of intracellular signals to modulate cell activation, differentiation, and survival (59). It is noteworthy that adding glycoproteins (such as PSM) that are good ligands for CvGal1 to attached and spread hemocytes promotes their activation and enhances phagocytosis of the parasite *P. marinus*, an observation that we have interpreted as the clustering of hemocyte bound CvGal1 by the multivalent glycoprotein.[5] The possibility that the hemocyte CvGal1 ligand responsible is in fact β-integrin allows the rationalization of the aforementioned outcome of a three-component glycoprotein-CvGal1-β-integrin lattice leading to cell activation.

In contrast with the evidence we obtained toward the identification of blood group A oligosaccharides as the CvGal1 ligands on the surface of the oyster hemocytes, similar studies aimed at the exploring the possibility that CvGal1 recognized blood group A oligosaccharides on the *P. marinus* trophozoite surface yielded very different results. Although glycotyping analysis of the parasite surface with labeled plant lectins indicated that GalNAc and Gal moieties recognized by SBA and PNA, respectively, are exposed on the parasite surface, based on the lack of binding of anti-A and anti-B monoclonal antibodies, these are not part of blood group A and B oligosaccharides but may still be effective ligands for CvGal1. Thus, we hypothesize that the parasite has evolved its glycocalyx to develop effective mimicry of the self-ligands recognized by CvGal1 on the hemocyte surface to gain entry into the oyster host, survive the oxidative attack, and proliferate (15). Because the blood group A oligosaccharide structures recognized on the hemocyte surface are not present on the parasite surface, the mimicry extends to

[5] S. Tasumi and G. R. Vasta, unpublished data.

the topology rather than the structure of the hemocyte glycans and is most likely the result of convergent evolution. It has been proposed that the ABH system in mammals is the evolutionary product of pathogen evasion strategies by the host prior to the advent of adaptive immune responses (38). If this is the case, the parasite *P. marinus* has effectively co-evolved with its bivalve host to display glycan-based mimicry and facilitate CvGal1-mediated recognition and entry (19).

Acknowledgments—We are grateful to Dr. David Smith and Dr. Jamie Molinaro from the Core H, Consortium for Functional Glycomics, Emory University, Atlanta, GA, for the glycan array analysis of CvGal1; Bob O'Meally from the Proteomics Core Facility at The Johns Hopkins University, Baltimore, MD, for the Mass Spectrometry Analysis of CvGal1 ligands, and Dr. Katharina Paschinger for critically reading the manuscript.

REFERENCES

1. Boehm, T. (2012) Evolution of vertebrate immunity. *Curr. Biol.* **22,** R722–R732
2. Vasta, G. R., Ahmed, H., and Odom, E. W. (2004) Structural and functional diversity of lectin repertoires in invertebrates, protochordates, and ectothermic vertebrates. *Curr. Opin. Struct. Biol.* **14,** 617–630
3. Schmitt, P., Rosa, R. D., Duperthuy, M., de Lorgeril, J., Bachre, E., and Destoumieux-Garzn, D. (2012) The antimicrobial defense of the Pacific oyster, *Crassostrea gigas.* How Diversity may compensate for scarcity in the regulation of resident/pathogenic microflora. *Front. Microbiol.* **3,** 160
4. Kennedy, V. S., Newell, R. I., and Eble, A. F. (eds) (1996) *The Eastern Oyster: Crassostrea virginica,* 2nd Ed., University of Maryland Sea Grant Publications
5. Dame, R., Bushek, D., Allen, D., Lewitus, A., Edwards, D., Koepfler, E., and Gregory, L. (2002) Ecosystem response to bivalve density reduction: management implications. *Aquat. Ecol.* **36,** 51–65
6. Vasta, G. R., Sullivan, J. T., Cheng, T. C., Marchalonis, J. J., and Warr, G. W. (1982) A cell membrane-associated lectin of the oyster hemocyte. *J. Invertebr. Pathol.* **40,** 367–377
7. Vasta, G. R., Cheng, T. C., and Marchalonis, J. J. (1984) A lectin on the hemocyte membrane of the oyster (*Crassostrea virginica*). *Cell Immunol.* **88,** 475–488
8. Andrews, J. D. (1996) History of *Perkinsus marinus*, a pathogen of oysters in Chesapeake Bay 1950–1984. *J. Shellfish Res.* **15,** 13–16
9. Harvell, C. D., Kim, K., Burkholder, J. M., Colwell, R. R., Epstein, P. R., Grimes, D. J., Hofmann, E. E., Lipp, E. K., Osterhaus, A. D., Overstreet, R. M., Porter, J. W., Smith, G. W., and Vasta, G. R. (1999) Emerging marine diseases–climate links and anthropogenic factors. *Science* **285,** 1505–1510
10. Perkins, F. O. (1996) The Structure of *Perkinsus marinus*, with comments on taxonomy and phylogeny of *Perkinsus* spp. *J. Shellfish Res.* **15,** 67–87
11. Cáceres-Martínez, J., Ortega, M. G., Vásquez-Yeomans, R., García Tde, J., Stokes, N. A., and Carnegie, R. B. (2012) Natural and cultured populations of the mangrove oyster *Saccostrea palmula* from Sinaloa, Mexico, infected by *Perkinsus marinus*. *J. Invertebr. Pathol.* **110,** 321–325
12. Bushek, D., Ford, S. E., and Chintala, M. M. (2002) Comparison of *in vitro*-cultured and wild-type *Perkinsus marinus.* III. Fecal elimination and its role in transmission. *Dis. Aquat. Org.* **51,** 217–225
13. Ford, S. E., Chintala, M. M., and Bushek, D. (2002) Comparison of *in vitro*-cultured and wild-type *Perkinsus marinus*. I. Pathogen virulence. *Dis. Aquat. Org.* **51,** 187–201
14. Chu, F.-L. (1996) Laboratory investigations of susceptibility, infectivity, and transmission of *Perkinsus marinus* in oysters. *J. Shellfish Res.* **15,** 57–66
15. Tasumi, S., and Vasta, G. R. (2007) A galectin of unique domain organization from hemocytes of the eastern oyster (*Crassostrea virginica*) Is a receptor for the protistan parasite *Perkinsus marinus*. *J. Immunol.* **179,** 3086–3098
16. Vasta, G. R., and Ahmed, H. (eds) (2008) *Animal Lectins: A Functional View*, CRC Press, Inc., Boca Raton, FL
17. Leffler, H., Carlsson, S., Hedlund, M., Qian, Y., and Poirier, F. (2004) Introduction to galectins. *Glycoconj. J.* **19,** 433–440
18. Rabinovich, G. A., and Croci, D. O. (2012) Regulatory circuits mediated by lectin-glycan interactions in autoimmunity and cancer. *Immunity* **36,** 322–335
19. Vasta, G. R. (2009) Roles of galectins in infection. *Nat. Rev. Microbiol.* **7,** 424–438
20. Medzhitov, R., and Janeway, C. A., Jr. (2002) Decoding the patterns of self and nonself by the innate immune system. *Science* **296,** 298–300
21. Vasta, G. R., Ahmed, H., Nita-Lazar, M., Banerjee, A., Pasek, M., Shridhar, S., Guha, P., and Fernández-Robledo, J. A. (2012) Galectins as self/non-self recognition receptors in innate and adaptive immunity: an unresolved paradox. *Front. Immunol.* **3,** 199
22. Fernández-Robledo, J. A., Lin, Z., and Vasta, G. R. (2008) Transfection of the protozoan parasite *Perkinsus marinus*. *Mol. Biochem. Parasitol.* **157,** 44–53
23. Gauthier, J. D., Vasta, G. R. (1995) *In vitro* culture of the eastern oyster parasite *Perkinsus marinus*: Optimization of the methodology. *J. Invertebr. Pathol.* **66,** 156–168
24. Bianchet, M. A., Ahmed, H., Vasta, G. R., and Amzel, L. M. (2000) Soluble β-galactosyl-binding lectin (galectin) from toad ovary: crystallographic studies of two protein-sugar complexes. *Proteins* **40,** 378–388
25. Emsley, P., and Cowtan, K. (2004) Coot: model-building tools for molecular graphics. *Acta Crystallogr. D Biol. Crystallogr.* **60,** 2126–2132
26. Ahmed, H., Bianchet, M. A., Amzel, L. M., Hirabayashi, J., Kasai, K., Giga-Hama, Y., Tohda, H., and Vasta, G. R. (2002) Novel carbohydrate specificity of the 16-kDa galectin from *Caenorhabditis elegans*: binding to blood group precursor oligosaccharides (type 1, type 2, Tα, and Tβ) and gangliosides. *Glycobiology* **12,** 451–461
27. Shevchenko, A., Wilm, M., Vorm, O., and Mann, M. (1996) Mass spectrometric sequencing of proteins silver-stained polyacrylamide gels. *Anal. Chem.* **68,** 850–858
28. Gettner, S. N., Kenyon, C., and Reichardt, L. F. (1995) Characterization of β pat-3 heterodimers, a family of essential integrin receptors in *C. elegans*. *J. Cell Biol.* **129,** 1127–1141
29. Pytela, R., Suzuki, S., Breuss, J., Erle, D. J., and Sheppard, D. (1994) Polymerase chain reaction cloning with degenerate primers: homology-based identification of adhesion molecules. *Method Enzymol.* **245,** 420–451
30. Thomsson, K. A., Karlsson, H., and Hansson, G. C. (2000) Sequencing of sulfated oligosaccharides from mucins by liquid chromatography and electrospray ionization tandem mass spectrometry. *Anal. Chem.* **72,** 4543–4549
31. Baenziger, J. U., and Fiete, D. (1979) Structure of the complex oligosaccharides of fetuin. *J. Biol. Chem.* **254,** 789–795
32. Gauthier, J. D., Jenkins, J. A., and La Peyre, J. F. (2004) Flow cytometric analysis of lectin binding to *in vitro*-cultured *Perkinsus marinus* surface carbohydrates. *J. Parasitol.* **90,** 446–454
33. Petri, W. A., Jr., Haque, R., and Mann, B. J. (2002) The bittersweet interface of parasite and host: lectin-carbohydrate interactions during human invasion by the parasite *Entamoeba histolytica*. *Annu. Rev. Microbiol.* **56,** 39–64
34. Hager, K. M., and Carruthers, V. B. (2008) MARveling at parasite invasion. *Trends Parasitol.* **24,** 51–54
35. Di Lella, S., Sundblad, V., Cerliani, J. P., Guardia, C. M., Estrin, D. A., Vasta, G. R., and Rabinovich, G. A. (2011) When galectins recognize glycans: from biochemistry to physiology and back again. *Biochemistry* **50,** 7842–7857
36. Stowell, S. R., Arthur, C. M., Mehta, P., Slanina, K. A., Blixt, O., Leffler, H., Smith, D. F., and Cummings, R. D. (2008) Galectin-1, -2, and -3 exhibit differential recognition of sialylated glycans and blood group antigens. *J. Biol. Chem.* **283,** 10109–10123
37. Stowell, S. R., Arthur, C. M., Slanina, K. A., Horton, J. R., Smith, D. F., and Cummings, R. D. (2008) Dimeric galectin-8 induces phosphatidylserine exposure in leukocytes through polylactosamine recognition by the C-terminal domain. *J. Biol. Chem.* **283,** 20547–20559

38. Stowell, S. R., Arthur, C. M., Dias-Baruffi, M., Rodrigues, L. C., Gourdine, J. P., Heimburg-Molinaro, J., Ju, T., Molinaro, R. J., Rivera-Marrero, C., Xia, B., Smith, D. F., and Cummings, R. D. (2010) Innate immune lectins kill bacteria expressing blood group antigen. *Nat. Med.* **16,** 295–301
39. Cooper, D. N., Boulianne, R. P., Charlton, S., Farrell, E. M., Sucher, A., and Lu, B. C. (1997) Fungal galectins, sequence and specificity of two isolectins from *Coprinus cinereus*. *J. Biol. Chem.* **272,** 1514–1521
40. Walser, P. J., Haebel, P. W., Künzler, M., Sargent, D., Kües, U., Aebi, M., and Ban, N. (2004) Structure and functional analysis of the fungal galectin CGL2. *Structure* **12,** 689–702
41. van den Berg, T. K., Honing, H., Franke, N., van Remoortere, A., Schiphorst, W. E., Liu, F. T., Deelder, A. M., Cummings, R. D., Hokke, C. H., and van Die, I. (2004) LacdiNAc-glycans constitute a parasite pattern for galectin-3-mediated immune recognition. *J. Immunol.* **173,** 1902–1907
42. Butschi, A., Titz, A., Wälti, M. A., Olieric, V., Paschinger, K., Nöbauer, K., Guo, X., Seeberger, P. H., Wilson, I. B., Aebi, M., Hengartner, M. O., and Künzler, M. (2010) *Caenorhabditis elegans N*-glycan core β-galactoside confers sensitivity toward nematotoxic fungal galectin CGL2. *PLoS Pathog.* **6,** e1000717
43. Wälti, M. A., Walser, P. J., Thore, S., Grünler, A., Bednar, M., Künzler, M., and Aebi, M. (2008) Structural basis for chitotetraose coordination by CGL3, a novel galectin-related protein from *Coprinopsis cinerea*. *J. Mol. Biol.* **379,** 146–159
44. Le Guyader, F. S., Bon, F., DeMedici, D., Parnaudeau, S., Bertone, A., Crudeli, S., Doyle, A., Zidane, M., Suffredini, E., Kohli, E., Maddalo, F., Monini, M., Gallay, A., Pommepuy, M., Pothier, P., and Ruggeri, F. M. (2006) Detection of multiple noroviruses associated with an international gastroenteritis outbreak linked to oyster consumption. *J. Clin. Microbiol.* **44,** 3878–3882
45. Tian, P., Engelbrektson, A. L., and Mandrell, R. E. (2008) Seasonal tracking of histo-blood group antigen expression and norovirus binding in oyster gastrointestinal cells. *J. Food Prot.* **71,** 1696–1700
46. Zhang, G., Fang, X., Guo, X., Li, L., Luo, R., Xu, F., Yang, P., Zhang, L., Wang, X., Qi, H., Xiong, Z., Que, H., Xie, Y., Holland, P. W., Paps, J., Zhu, Y., Wu, F., Chen, Y., Wang, J., Peng, C., Meng, J., Yang, L., Liu, J., Wen, B., Zhang, N., Huang, Z., Zhu, Q., Feng, Y., Mount, A., Hedgecock, D., Xu, Z., Liu, Y., Domazet-Lošo, T., Du, Y., Sun, X., Zhang, S., Liu, B., Cheng, P., Jiang, X., Li, J., Fan, D., Wang, W., Fu, W., Wang, T., Wang, B., Zhang, J., Peng, Z., Li, Y., Li, N., Wang, J., Chen, M., He, Y., Tan, F., Song, X., Zheng, Q., Huang, R., Yang, H., Du, X., Chen, L., Yang, M., Gaffney, P. M., Wang, S., Luo, L., She, Z., Ming, Y., Huang, W., Zhang, S., Huang, B., Zhang, Y., Qu, T., Ni, P., Miao, G., Wang, J., Wang, Q., Steinberg, C. E., Wang, H., Li, N., Qian, L., Zhang, G., Li, Y., Yang, H., Liu, X., Wang, J., Yin, Y., and Wang, J. (2012) The oyster genome reveals stress adaptation and complexity of shell formation. *Nature* **490,** 49–54
47. Itoh, N., Xue, Q. G., Schey, K. L., Li, Y., Cooper, R. K., and La Peyre, J. F. (2011) Characterization of the major plasma protein of the eastern oyster, *Crassostrea virginica*, and a proposed role in host defense. *Comp. Biochem. Physiol. B Biochem. Mol. Biol.* **158,** 9–22
48. Schott, E. J., and Vasta, G. R. (2003) The PmSOD1 gene of the protistan parasite *Perkinsus marinus* complements the sod2Δ mutant of *Saccharomyces cerevisiae* and directs an iron superoxide dismutase to mitochondria. *Mol. Biochem. Parasitol.* **126,** 81–92
49. Schott, E. J., Robledo, J. A., Wright, A. C., Silva, A. M., and Vasta, G. R. (2003) Gene organization and homology modeling of two iron superoxide dismutases of the early branching protist *Perkinsus marinus*. *Gene* **309,** 1–9
50. Fernández-Robledo, J. A., Schott, E. J., and Vasta, G. R. (2008) *Perkinsus marinus* superoxide dismutase 2 (PmSOD2) localizes to single-membrane subcellular compartments. *Biochem. Biophys. Res. Commun.* **375,** 215–219
51. Alavi, M. R., Fernández-Robledo, J. A., and Vasta, G. R. (2009) Development of an *in vitro* assay to examine intracellular survival of *Perkinsus marinus* trophozoites upon phagocytosis by oyster (*Crassostrea virginica* and *Crassostrea ariakensis*) hemocytes. *J. Parasitol.* **95,** 900–907
52. Robledo, J. A., Courville, P., Cellier, M. F., and Vasta, G. R. (2004) Gene organization and expression of the divalent cation transporter Nramp in the protistan parasite *Perkinsus marinus*. *J. Parasitol.* **90,** 1004–1014
53. Lin, Z., Fernández-Robledo, J. A., Cellier, M. F., and Vasta, G. R. (2011) The natural resistance-associated macrophage protein from the protozoan parasite *Perkinsus marinus* mediates iron uptake. *Biochemistry* **50,** 6340–6355
54. Cellier, M. F., Courville, P., and Campion, C. (2007) Nramp1 phagocyte intracellular metal withdrawal defense. *Microbes Infect.* **9,** 1662–1670
55. Orsi, N. (2004) The antimicrobial activity of lactoferrin: current status and perspectives. *Biometals* **17,** 189–196
56. Zhuo, Y., Chammas, R., and Bellis, S. L. (2008) Sialylation of β1 integrins blocks cell adhesion to galectin-3 and protects cells against galectin-3-induced apoptosis. *J. Biol. Chem.* **283,** 22177–22185
57. Lim, J., and Hotchin, N. A. (2012) Signalling mechanisms of the leukocyte integrin αMβ2: current and future perspectives. *Biol. Cell* **104,** 631–640
58. Mayadas, T. N., and Cullere, X. (2005) Neutrophil β2 integrins: moderators of life or death decisions. *Trends Immunol.* **26,** 388–395
59. Rabinovich, G. A., Toscano, M. A., Jackson, S. S., and Vasta, G. R. (2007) Functions of cell surface galectin-glycoprotein lattices. *Curr. Opin. Struct. Biol.* **17,** 513–520
60. Risler, J. L., Delorme, M. O., Delacroix, H., and Henaut, A. (1988) Amino acid substitutions in structurally related proteins. A pattern recognition approach. Determination of a new and efficient scoring matrix. *J. Mol. Biol.* **204,** 1019–1029
61. Kurz, S., Jin, C., Hykollari, A., Gregorich, D., Giomarelli, B., Vasta, G. R., Wilson, I. B. H., and Paschinger, K. (2013) Hemocytes and plasma of the eastern oyster (*Crassostrea virginica*) display a diverse repertoire of sulfated and blood group A-modified *N*-glycans. *J. Biol. Chem.* 24410–24428